Science
AAAS

Title:

Peritumoral activation of the Hippo pathway effectors Yap and Taz suppresses liver cancer in mice

Authors:

Iván M. Moya[ab#], Stéphanie A. Castaldo[a#], Laura Van den Mooter[a#], Soheil Soheily[a#], Leticia Sansores-Garcia[a], Jelle Jacobs[c], Inge Mannaerts[d], Jun Xie[a], Elisabeth Verboven[a], Hanne Hillen[a], Ana Algueró-Nadal[a], Ruchan Karaman[a], Matthias Van Haele[e], Weronika Kowalczyk[a], Maxime De Waegeneer[c], Stefaan Verhulst[d], Panagiotis Karras[f], Leen van Huffel[a], Lars Zender[h], Jean-Christophe Marine[f], Tania Roskams[e], Randy Johnson[g], Stein Aerts[c], Leo A. van Grunsven[d], and Georg Halder[a*]

Affiliations:

[a] VIB Center for Cancer Biology and KU Leuven Department of Oncology, University of Leuven, Leuven, Belgium

[b] Facultad de Ingeniería y Ciencias Aplicadas. Universidad de Las Americas, Quito. Ecuador.

[c] VIB Center for Brain and Disease Research and KU Leuven Center for Human Genetics, University of Leuven, Leuven, Belgium

[d] Liver Cell Biology research group, Vrije Universiteit Brussel, 1090 Brussel, Belgium

[e] Department of Imaging and Pathology, KU Leuven and University Hospitals Leuven, Leuven, Belgium

[f] Laboratory for Molecular Cancer Biology, VIB Center for Cancer Biology and Department of Oncology, KU Leuven, Leuven, Belgium

[g] Department of Cancer Biology, Program in Cancer Biology, Graduate School for Biological Sciences GSBS, The University of Texas MD Anderson Cancer Center, Houston, Texas, USA

[h] 1) Department of Medical Oncology and Pneumology, University Hospital Tuebingen, 72076 Tuebingen, Germany. 2) German Cancer Research Consortium (DKTK), German Cancer Research Center (DKFZ), 69120 Heidelberg, Germany. 3) iFIT Cluster of Excellence EXC 2180 “Image Guided and Functionally Instructed Tumour Therapies“, University of Tuebingen, Tuebingen, Germany

[#] Equal contribution

[*] Corresponding author. Email: Georg.Halder@vib.be.

Abstract:

The Hippo signaling pathway and its two downstream effectors, the Yap and Taz transcriptional co-activators, are drivers of tumor growth in experimental models. Studying mouse models, we show that Yap/Taz can also exert a tumor suppressive function. We found that normal hepatocytes surrounding liver tumors display activation of Yap/Taz and that deletion of *Yap/Taz* in these peritumoral hepatocytes accelerated tumor growth. Conversely, experimental hyperactivation of Yap in peritumoral hepatocytes triggered regression of primary liver tumors and melanoma-derived liver metastases. Furthermore, whereas tumor cells growing in wild-type livers required Yap/Taz for their survival, those surrounded by *Yap/Taz*-deficient hepatocytes were not dependent on Yap/Taz. Tumor cell survival thus depends on the relative activity of Yap/Taz in tumor cells and their surrounding tissue, suggesting that Yap and Taz act through a mechanism of cell competition to eliminate tumor cells.

Main Text:

The Hippo signaling pathway has been implicated in cancer development in humans and mice. Its two downstream effectors, the homologous YAP and TAZ transcriptional co-activators, are upregulated in a wide range of human cancers (*1, 2*). When active, YAP and TAZ accumulate in the nucleus and through their binding to transcription factors such as TEAD, they regulate the expression of target genes that promote cell proliferation, stemness and cell survival. Their hyperactivation can thus trigger the expansion of progenitor cell populations, induce organ overgrowth, and lead to cancer initiation (*2, 3*). YAP and TAZ are considered attractive targets for cancer therapy because they are required for the proliferation and survival of cancer cells while being largely dispensable for homeostasis of many adult mouse tissues (*1-3*). However, little is known about the function of YAP and TAZ in normal cells of the immediate and larger tumor environment.

To study the function of the Hippo pathway in tumor and peritumoral cells, we induced the development of intrahepatic cholangiocarcinoma (CCA) in adult mice by hydrodynamic tail vein injection of genome-integrating sleeping beauty (SB) plasmids that express activated versions of the Notch receptor (myc-tagged Notch intracellular domain, N^{ICD}) and Akt (myristoylated and HA-tagged, HA-Akt) (*4*). This procedure results in transfection of scattered hepatocytes and leads to multiple macroscopic tumors 6 to 7 weeks after DNA injection into C57BL/6 mice (fig. S1), hereafter referred to as N-Akt tumors) (*4*). High levels of Yap and Taz were present in N-Akt tumor cells (Fig. 1A and fig. S2A) as is seen in human cholangiocarcinoma (*5*). Yap levels in

tumor cells were as high as those in bile duct and endothelial cells where Yap is normally expressed (Fig. 1A) (*6, 7*).

We also observed Yap accumulation in hepatocytes around N-Akt tumors; in contrast, Yap was barely detectable in hepatocytes of normal livers (Fig. 1A). This accumulation of Yap in peritumoral hepatocytes was not due to direct effects of N^{ICD} or HA-Akt expression in these cells, because all peritumoral hepatocytes showed Yap accumulation while only few of them expressed N^{ICD} or HA-Akt (fig. S2B-C). Moreover, N^{ICD} or HA-Akt expression alone was not sufficient to induce Yap accumulation in peritumoral hepatocytes (fig. S2D). Yap accumulation was not due to elevated levels of *Yap* mRNA in hepatocytes (fig. S2E) but to posttranslational regulation because the presence of N-Akt tumors triggered nuclear accumulation of ectopically expressed HA-tagged Yap in peritumoral hepatocytes (Fig. 1B and C).

We also observed YAP and TAZ accumulation in peritumoral hepatocytes of about 50% of human hepatocellular carcinoma (HCC, 44 out of 82) and CCA (13 out of 26), but not in hepatocytes of healthy human livers (fig. S3). Nearly all of these patients showed strong YAP nuclear accumulation in peritumoral hepatocytes (fig. S4). In addition, YAP accumulated in peritumoral zones of colorectal cancer and melanoma metastases to the liver (fig. S5). Notably, unlike most primary liver cancers, these metastases occurred in normal livers, demonstrating that the activation of YAP was due to the tumor and not to underlying liver disease.

To address whether Yap/Taz were active in peritumoral hepatocytes, we studied the gene expression profiles of purified hepatocytes from normal livers and livers with N-Akt tumors by RNA-seq (fig. S6A-C, see Methods). This identified 3273 and 523 genes that were significantly up or downregulated, respectively (log2FC>1, FDR<0.05). The upregulated genes were enriched for those encoding factors functioning in cell proliferation, stress response, and wound healing (fig. S6D) and gene set enrichment analysis (GSEA) detected prominent Hippo pathway gene expression signatures (*8-10*) (NES=2.57 and 2.33, FDR<0.05) (Fig. 1D and E). Among the upregulated genes were classic Yap targets including *Ctgf, Cyr61, Pdgfr, Fbn1, Ankrd1,* and *Birc5*, which was confirmed by quantitative reverse transcriptase-PCR (qRT-PCR) (Fig. 1D and F). Consistent with Yap activation, about 6% of peritumoral hepatocytes expressed a marker of cell proliferation ($HNF4a^{+}$ $Ki67^{+}$) in tumor-bearing livers, whereas less than 0.2% of hepatocytes expressed Ki67 in normal livers (fig. S7). These data show that Yap/Taz were ectopically activated in peritumoral hepatocytes.

To determine the function of the Hippo pathway in peritumoral hepatocytes, we simultaneously deleted *Yap* and its redundantly acting homolog *Taz* in hepatocytes but not in tumor cells. This was achieved by injecting a Cre expressing adeno-associated virus 8 (AAV-Cre) into $Yap^{fl/fl};Taz^{fl/fl}$ double floxed mice (*11, 12*) that had N-Akt tumors (Fig. 2A). AAV-Cre expresses Cre under the hepatocyte-specific Thyroxine-binding globulin (TBG) promoter (*4, 13*) and its injection into *R26-LoxP-STOP-LoxP-tdTomato* reporter mice bearing N-Akt tumors triggered recombination of the *tdTomato* reporter in essentially all hepatocytes but in less than 0.05% of cholangiocarcinoma cells (fig. S8A-D). AAV-Cre was administered 4 weeks after N^{ICD}

and *HA-Akt* plasmid injection and mice were analyzed three weeks later (Fig. 2A). Analysis of *Yap* and *Taz* mRNA and protein levels confirmed robust deletion in peritumoral hepatocytes (fig. S8E and F). Strikingly, deletion of *Yap*/*Taz* in peritumoral hepatocytes resulted in increased tumor burden (Fig. 2B-E). We established this by quantifying the relative tumor area on liver sections (excluding the tumor luminal spaces) and by determining the absolute tumor mass (by multiplying the relative tumor area with the liver weight) (Fig. 2B-D). The increase in tumor burden was due to an increase in tumor cell proliferation, as evidenced by the increased number of Ki67-positive tumor cells (Fig. 2F and G). This effect was a result of *Yap*/*Taz* deletion and not to nonspecific effects of AAV-Cre infection because AAV-Cre injection did not affect tumor burden in C57BL/6 control mice (fig. S9). These data highlight an unexpected activity of Yap/Taz in peritumoral hepatocytes that non-autonomously restrains tumor growth.

The finding that endogenous activation of Yap/Taz in peritumoral hepatocytes restrains tumor growth prompted us to test whether additional activation of Yap/Taz in peritumoral hepatocytes could cause tumor elimination. To study this question, we activated Yap/Taz by conditional deletion of the genes encoding the upstream Large tumor suppressor kinases 1/2 (Lats1/2), which inhibit Yap/Taz by phosphorylation (*3*). We injected the N^{ICD} and *HA-Akt* plasmid into $Lats1^{fl/fl};Lats2^{fl/fl}$ double floxed mice (*14*) and triggered *Lats1/2* deletion in peritumoral hepatocytes by AAV-Cre injection four weeks later when livers already had macroscopic tumors (Fig.3A and fig. S10A). Peritumoral deletion of *Lats1/2* caused a decrease in phospho-S112-Yap, an increase in Taz (fig. S10B), strong activation of hepatocyte proliferation

(fig. S10C and D), and liver overgrowth (Fig. 3B). Thus, deletion of *Lats1/2* hyperactivated Yap/Taz above the levels present in wild-type peritumoral hepatocytes.

Two weeks after *Lats1/2* deletion, most mutant livers showed dramatically reduced tumor load compared to controls (Fig. 3C-E). In control mice, tumors occupied 40% of the liver volume whereas in mice with *Lats1/2* mutant livers, tumors occupied less than 5% of the liver volume (fig. S10E). This represents a greater than 70% reduction in tumor load (Fig. 3C). This effect was mediated by Yap/Taz as simultaneous deletion of *Yap, Taz, Lats1,* and *Lats2* in peritumoral hepatocytes abolished the ectopic hepatocyte proliferation and tumor elimination observed upon *Lats1/2* deletion (Fig.3B and C; fig. S10C-E). This experiment confirmed that Yap/Taz act as tumor suppressors in peritumoral hepatocytes because mice with *Yap, Taz, Lats1/2* quadruple mutant hepatocytes had increased cancer cell proliferation and tumor burden when compared to non-AAV-Cre injected siblings (fig. S10F-L).

In a second approach to activate Yap/Taz in peritumoral hepatocytes, we used transgenic mice that conditionally overexpress a constitutively active form of human YAP ($hYAP^{1SA}$), which contains a mutation of the major Lats1/2 phosphorylation site, under the doxycycline (Dox) inducible TetON system (*15*). These mice showed induced expression of $hYAP^{1SA}$ specifically in hepatocytes but not in cholangiocytes (fig. S11A) because they express the reverse tetracycline transactivator (rtTA) under the hepatocyte-specific *ApoE* promoter (hereafter called *Apo>hYAP*^{1SA})(*15*). Indeed, Dox feeding led to an increase in YAP protein levels (fig. S11B) and induced hepatocyte proliferation and liver overgrowth in *Apo>hYAP*^{1SA} mice (fig. S11C-E) (*15*).

We next induced N-Akt tumors in *Apo>hYAP^{1SA}* mice and activated hYAP^{1SA} expression at week 4 of tumor development by adding Dox to their drinking water (fig. S11F). Two weeks later, these mice displayed a prominent reduction in tumor load compared to non-treated *Apo>hYAP^{1SA}* siblings and Dox treated C57BL/6 mice with N-Akt tumors (Fig. 3F; fig. S11G-I). Mice that were fed Dox for 2 weeks had extended survival, although they eventually died from recurrent cholangiocarcinoma (Fig. 3G). Thus, ectopic Yap activation in peritumoral hepatocytes is sufficient to induce tumor regression.

To investigate whether tumor elimination is due simply to peritumoral hepatocyte overproliferation, we simultaneously overexpressed oncogenic BRaf^{V600E} and deleted *PTEN* in peritumoral hepatocytes to trigger ectopic hepatocyte proliferation (*16*). While *BRaf^{V600E};PTEN^{CKO}* livers overgrew at the same rate and to the same size as *Apo>hYAP^{1SA}* livers, this did not affect N-Akt tumor growth (fig. S12). Thus, tumor elimination is not caused by excessive proliferation of peritumoral hepatocytes, but is a specific effect driven by Yap/Taz activation.

The decrease in tumor burden was likely due to the elimination of tumor cells by programmed cell death (PCD). N-Akt tumors surrounded by *Lats1/2* mutant or hYAP^{1SA} expressing hepatocytes had more cells that were positive for TUNEL staining (which labels fragmented DNA in dying cells) (Fig. 4A and B; fig. S13A) but displayed no change in proliferation (fig. S13B and C). Regressing tumors had lower levels of the anti-apoptotic protein Bcl2 compared to tumors from control mice (Fig. 4C), but there were no significant increases in cleaved Caspase3,

Poly[ADP-ribose] polymerase 1 (PARP-1), tumor hypoxia (Hif2A, Glut1), phosphorylated RIPK3 or p38, and immune cell infiltration (CD45 and CD3; fig. S13D and E). Nor were there decreases in readouts for nutrient status of tumor cells such as phosphorylated S6, Akt, and AMPK, or growth factor signaling (phosphorylated ERK) (Fig. 4C; fig. S13G and H). We also did not observe substantial changes in the amounts of Yap, Taz, and phosphorylated Yap compared to control tumors (Fig. 4D), thus excluding the possibility that tumor regression was due to feedback inhibition of the Hippo pathway. Notably, Dox-induced conditional overexpression of Bcl2 in tumor cells, starting at the time of *Lats1/2* deletion or $hYAP^{1SA}$ overexpression in surrounding hepatocytes, abolished tumor elimination (fig. S14; fig. S15; see Methods). Thus, Yap/Taz activation in peritumoral hepatocytes triggers non-apoptotic programmed cell death in tumor cells, which is prevented by Bcl2 overexpression.

The finding that Yap-activated hepatocytes can suppress the growth of liver tumors suggested a competitive interaction between tumor cells and their surrounding tissue. We thus investigated how Yap and Taz affects the competitive fitness of established tumors against peritumoral hepatocytes. First, we deleted *Yap* and *Taz* in tumor cells but not in surrounding hepatocytes. We co-injected a plasmid that expressed the tamoxifen inducible Cre^{ERT2} (*SB-*Cre^{ERT2}) together with the N^{ICD} and *HA-Akt* plasmids into $Yap^{fl/fl}$;$Taz^{fl/fl}$ double floxed mice, and then triggered *Yap/Taz* deletion by tamoxifen administration four weeks later, when macroscopic tumors had formed (fig. S16A). Deletion of *Yap* and *Taz* in tumor cells strongly reduced tumor burden (Fig. 4E-H). Three weeks after *Yap/Taz* deletion, no macroscopic tumors were visible and the liver parenchyma was largely composed of normal hepatocytes and contained only a few tumor

remnants (Fig. 4E). As controls, tamoxifen injection did not affect tumor burden in wild-type C57BL/6 mice that had *SB-Cre*^{ERT2} expressing N-Akt tumors and in *Yap*$^{fl/fl}$;*Taz*$^{fl/fl}$ mice with N-Akt tumors that did not have *SB-Cre*^{ERT2} (fig. S9). Thus, Yap and Taz are required for N-Akt tumor maintenance when surrounded by wild-type hepatocytes.

In a second experiment we simultaneously deleted *Yap* and *Taz* in tumor cells and in peritumoral hepatocytes. To do this, we co-injected *SB-Cre*^{ERT2} together with the *N*^{ICD} and *HA-Akt* plasmids into *Yap*$^{fl/fl}$;*Taz*$^{fl/fl}$ mice as above but then injected tamoxifen together with AAV-Cre four weeks after plasmid injection (fig. S16A). Monitoring of Cre activity with the *Rosa26-LoxP-STOP-LoxP-tdTomato* reporter confirmed ubiquitous tdTomato expression in virtually all tumor cells and peritumoral hepatocytes (fig. S16B). Efficient reduction of Yap/Taz protein in tumor cells and normal hepatocytes was confirmed by immunohistochemistry and western blot (fig. S16C and D). Cell death was reduced in *Yap/Taz* mutant N-Akt tumors and the tumor cells proliferated when surrounded by *Yap/Taz* mutant hepatocytes (Fig. 4E-H; fig. S16E and F). Thus, N-Akt tumor cells required Yap/Taz for survival, but only when surrounded by wild-type hepatocytes.

Finally we examined whether this tumor suppressor mechanism impacts the survival of other types of liver tumors. We tested the effects of peritumoral Yap activation on mouse hepatocellular carcinoma induced by co-expressing *Myc* and *NRas*^{G12V} (*17*) (hereafter called Myc-Ras tumors), in *Apo>hYAP*^{1SA} mice. To prevent *hYAP*^{1SA} expression in Myc-Ras tumor cells, we co-injected plasmids expressing shRNAs targeting the *rtTA* and *hYAP*^{1SA} transgenes together

with the *Myc* and *NRas*^{G12V} plasmids (fig. S17; fig. S18)(*18*). Notably, the *YAP*^{1SA} transgene encodes human YAP, which allowed us to design shRNAs that specifically target the human *YAP*^{1SA} transgene but not the endogenous mouse *Yap* gene. Control mice expressing *Myc-Ras* and shRNAs targeting *rtTA* and *hYAP,* but that did not receive Dox*,* developed a high tumor load 6 to 7 weeks after plasmid injection (fig. 4I and J). In contrast, Dox treated *Apo>hYAP*^{1SA} mice expressing the *rtTA* or *hYAP* shRNA had reduced tumor loads and mice expressing both shRNAs showed nearly complete tumor elimination (Fig. 4I and J; fig. S17; fig. S18). Therefore, YAP activation in peritumoral hepatocytes is sufficient to eliminate hepatocellular carcinoma.

Many types of cancer metastasize to the liver (*19*). Melanoma liver metastases are lethal, especially for patients whose tumors harbor an activating *RAS* mutation. To test whether Yap-driven cell competition in hepatocytes can suppress the growth of such aggressive metastatic melanomas, we injected syngeneic mouse melanoma cells with an activating *NRAS* mutation and a deletion that abrogates *p16Ink4A* expression by hydrodynamic tail vein injection into *Apo>hYAP*^{1SA} mice. Hydrodynamic injection of tumor cells is highly effective in establishing tumor growth in the liver (*20*). Mice injected with 10^4 melanoma cells developed macroscopic tumors after 5 weeks and had to be euthanized after 7 weeks (Fig. 4K). We administered Dox in drinking water 3 weeks after the cell injection to induce hYAP^{1SA} expression in hepatocytes (fig. S19A). Two weeks after YAP activation, the *Apo>YAP*^{1SA} mice showed a 98% reduction in tumor load (Fig. 4K and L; fig. S19B-D). These melanoma lesions did not trigger endogenous Yap activation in peritumoral hepatocytes. Consistent with this, *Yap/Taz* deletion in peritumoral

hepatocytes did not alter melanoma growth in the liver (fig. S19E-J). Thus, YAP activated hepatocytes can outcompete highly aggressive NRAS-mutant melanoma cells.

The tumor suppression effect described here is reminiscent of "cell competition," a phenomenon originally described in *Drosophila* but recently also observed in mammalian systems (*21, 22*). During competition, intact viable cells are eliminated from a tissue when they are adjacent to cells that have higher fitness (referred to as winner and loser cells) (*21, 22*). Notably, winner or loser status is not an inherent property of a cell but can change upon alterations in the neighboring cells. In *Drosophila* imaginal discs, for instance, wild-type cells are winners when confronting Myc deficient cells but are losers when confronted with cells that overexpress Myc, a condition that converts cells into super-competitors (*23, 24*). Thus it is the relative level, not the absolute level, of Myc that determines winner/loser fate. Similarly, the reliance of liver tumor cells on Yap/Taz for their survival was not absolute, but relative to the levels of Yap/Taz in neighboring hepatocytes. Tumor cells died when surrounded by hepatocytes that had higher levels of Yap/Taz activity but survived when competition was neutralized -- for example, when tumor cells and hepatocytes simultaneously deleted *Yap/Taz* or when both overexpressed $hYAP^{1SA}$ such as in the shRNA control mice of the Apo>$hYAP^{1SA}$ experiment with Myc-Ras tumors (fig. S18B-D). Thus, a major function of Yap/Taz in tumor cells is to elevate their competitive fitness and to protect them from the tumor suppressive action of the surrounding parenchyma.

In summary, we have identified in our mouse models a mechanism of non-cell autonomous tumor suppression driven by the Hippo pathway effectors Yap and Taz, whereby the normal tissue surrounding liver tumors suppresses tumor growth and can cause its regression. Notably, this mechanism of tumor elimination is different from other previously described cell autonomous tumor suppressive functions of Yap/Taz (*25-27*), as here, Yap and Taz act non-cell autonomously in normal peritumoral cells and not by direct regulation of target genes in cancer cells. Whether analogous tumor suppressive mechanisms operate in human liver - or in other mouse organs -- is unknown. Given that YAP and TAZ are hyperactivated in many human cancers (*2*), there is a growing interest in developing drugs that inhibit YAP/TAZ as a possible cancer treatment. The data from the mouse models studied here raise the possibility that systemic inhibition of YAP/TAZ could have undesirable pro-tumorigenic effects.

REFERENCES AND NOTES

1. K. F. Harvey, X. Zhang, D. M. Thomas, The Hippo pathway and human cancer. *Nat Rev Cancer* **13**, 246-257 (2013).
2. T. Moroishi, C. G. Hansen, K. L. Guan, The emerging roles of YAP and TAZ in cancer. *Nat Rev Cancer* **15**, 73-79 (2015).
3. R. Johnson, G. Halder, The two faces of Hippo: targeting the Hippo pathway for regenerative medicine and cancer treatment. *Nat Rev Drug Discov* **13**, 63-79 (2014).
4. B. Fan *et al.*, Cholangiocarcinomas can originate from hepatocytes in mice. *The Journal of Clinical Investigation* **122**, 2911-2915 (2012).
5. P. Marti *et al.*, YAP promotes proliferation, chemoresistance, and angiogenesis in human cholangiocarcinoma through TEAD transcription factors. *Hepatology* **62**, 1497-1510 (2015).
6. N. Zhang *et al.*, The Merlin/NF2 tumor suppressor functions through the YAP oncoprotein to regulate tissue homeostasis in mammals. *Dev Cell* **19**, 27-38 (2010).
7. X. Wang *et al.*, YAP/TAZ Orchestrate VEGF Signaling during Developmental Angiogenesis. *Dev Cell* **42**, 462-478.e467 (2017).
8. M. Cordenonsi *et al.*, The Hippo transducer TAZ confers cancer stem cell-related traits on breast cancer cells. *Cell* **147**, 759-772 (2011).

9. B. J. Pepe-Mooney *et al.*, Single-Cell Analysis of the Liver Epithelium Reveals Dynamic Heterogeneity and an Essential Role for YAP in Homeostasis and Regeneration. *Cell Stem Cell*, (2019).
10. B. H. Sohn *et al.*, Inactivation of Hippo Pathway Is Significantly Associated with Poor Prognosis in Hepatocellular Carcinoma. *Clin Cancer Res* **22**, 1256-1264 (2016).
11. M. Xin *et al.*, Regulation of insulin-like growth factor signaling by Yap governs cardiomyocyte proliferation and embryonic heart size. *Sci Signal* **4**, ra70 (2011).
12. M. Xin *et al.*, Hippo pathway effector Yap promotes cardiac regeneration. *Proceedings of the National Academy of Sciences* **110**, 13839-13844 (2013).
13. K. Yanger *et al.*, Robust cellular reprogramming occurs spontaneously during liver regeneration. *Genes Dev* **27**, 719-724 (2013).
14. J. Yi *et al.*, Large tumor suppressor homologs 1 and 2 regulate mouse liver progenitor cell proliferation and maturation through antagonism of the coactivators YAP and TAZ. *Hepatology* **64**, 1757-1772 (2016).
15. J. Dong *et al.*, Elucidation of a universal size-control mechanism in Drosophila and mammals. *Cell* **130**, 1120-1133 (2007).
16. C. Kohler *et al.*, Mouse Cutaneous Melanoma Induced by Mutant BRaf Arises from Expansion and Dedifferentiation of Mature Pigmented Melanocytes. *Cell Stem Cell* **21**, 679-693.e676 (2017).
17. M. Seehawer *et al.*, Necroptosis microenvironment directs lineage commitment in liver cancer. *Nature* **562**, 69-75 (2018).
18. C. Fellmann *et al.*, An Optimized microRNA Backbone for Effective Single-Copy RNAi. *Cell Reports* **5**, 1704-1713 (2013).
19. S. S. Agarwala, A. M. Eggermont, S. O'Day, J. S. Zager, Metastatic melanoma to the liver: a contemporary and comprehensive review of surgical, systemic, and regional therapeutic options. *Cancer* **120**, 781-789 (2014).
20. J. Li, Q. Yao, D. Liu, Hydrodynamic cell delivery for simultaneous establishment of tumor growth in mouse lung, liver and kidney. *Cancer biology & therapy* **12**, 737-741 (2011).
21. R. Nagata, T. Igaki, Cell competition: Emerging mechanisms to eliminate neighbors. *Development, growth & differentiation* **60**, 522-530 (2018).
22. T. Maruyama, Y. Fujita, Cell competition in mammals - novel homeostatic machinery for embryonic development and cancer prevention. *Curr Opin Cell Biol* **48**, 106-112 (2017).
23. C. de la Cova, M. Abril, P. Bellosta, P. Gallant, L. A. Johnston, Drosophila myc regulates organ size by inducing cell competition. *Cell* **117**, 107-116 (2004).
24. E. Moreno, K. Basler, dMyc Transforms Cells into Super-Competitors. *Cell* **117**, 117-129 (2004).
25. S. Strano *et al.*, The transcriptional coactivator Yes-associated protein drives p73 gene-target specificity in response to DNA Damage. *Molecular cell* **18**, 447-459 (2005).
26. M. Yuan *et al.*, Yes-associated protein (YAP) functions as a tumor suppressor in breast. *Cell death and differentiation* **15**, 1752-1759 (2008).
27. E. R. Barry *et al.*, Restriction of intestinal stem cell expansion and the regenerative response by YAP. *Nature* **493**, 106-110 (2013).
28. B. Zhao *et al.*, TEAD mediates YAP-dependent gene induction and growth control. *Genes Dev* **22**, 1962-1971 (2008).

ACKNOWLEDGMENTS

We thank X. Chen, P. Hackett, C. Der, C. Distelhorst, and E.Kowarz for depositing plasmids at Addgene. We thank D.Pan for the *Apo>hYAP*^{1SA} mouse strain.

Funding: S.A.C., L.V.M. and E.V. were supported by a doctoral fellowship from the Research Foundation Flanders (FWO). I.M. was supported by a post-doctoral fellowship from FWO. L.Z. was supported by the German Research Foundation: DFG EXC 2180 – 390900677 [Image Guided and Functionally Instructed Tumour Therapies (iFIT)], FOR2314, SFB-TR209, Gottfried Wilhelm Leibniz Program], the German Ministry for Education and Research (BMBF): eMed/Multiscale HCC, the European Research Council: Consolidator grant 'CholangioConcept' and the German Center for Translational Cancer Research (DKTK). L.A.v.G and G.H. were supported by grants from FWO and G.H. by a grant from Stichting tegen Kanker (FAF-F/2016/867).

Author contributions: I.M.M., S.A.C., L.V.D.M., S.S., L.S.G., I.M., J.X., E.V., H.H., A.A.N., R.K., M.V.H., S.V., P.K. and L.V.H. conducted experiments. J.J., M.D.W., W.K. and S.A. conducted bioinformatics analyses and provided conceptual advice. T.R. performed pathology analysis and provided conceptual advice. R.J. provided genetic strains of mice. L.Z. provided genetic tools and conceptual advice. L.A.v.G and J.C.M edited the manuscript and provided conceptual advice. I.M.M. and G.H. designed the study and wrote the manuscript.

Competing interests: G.H. and I.M.M. are co-inventors of a patent ("Cancer regression by inducing a regeneration-like response, GB 1819659.2) filed by the VIB and KU University of Leuven.

Data and materials availability: The accession number for the cell sequencing datasets reported in this paper is GEO: GSE103788. The *Apo>hYAP*^{1SA} mouse strain is available from D. Pan at the University of Texas Southwestern Medical Center in Dallas under a material transfer agreement with the Johns Hopkins University, Baltimore; Mice carrying the *Yap and Taz* floxed alleles are available from E. Olson under a material transfer agreement with the University of Texas Southwestern Medical Center in Dallas.

SUPPLEMENTARY MATERIALS:

Materials and Methods

Figures S1 to S19

Figure Legends

Fig. 1. Yap is upregulated in peritumoral hepatocytes.

(A) Immunofluorescent detection of Yap on sections of wild-type mouse livers and livers with N-Akt tumors. Tumor cells were detected by HA-Akt expression (red). Arrows and arrowheads indicate Yap in bile duct and portal vein cells, respectively. (B-C) Immunofluorescent images and quantification of the localization of ectopically expressed HA-tagged Yap, 2 days after transfection into a few hepatocytes of normal livers and livers with N-Akt tumors. (D) Heat map

showing upregulation of global Yap signature genes *(10)* in peritumoral hepatocytes relative to hepatocytes from normal livers. (E) GSEA plots showing the distribution of two other more inclusive sets of Yap signature genes identified from human HCC samples *(10)* and cultured cells overexpressing YAP (*28*). (F) Quantitative RT-PCR for Yap/Taz target genes in purified normal and peritumoral hepatocytes. Data are Mean ± SEM. Scale bars 100μm. * = p<0.05, ** = p<0.01, *** = p<0.001 here and in all other figures; n.s. = not significant.

Fig. 2. Yap/Taz in peritumoral hepatocytes restrain tumor growth.

(A) Experimental outline: *Yap*$^{fl/fl}$*;Taz*$^{fl/fl}$ mice were hydrodynamically injected with *N*^{ICD}*, HA-Akt* and *SB11* plasmids. After four weeks, half of these mice were injected with AAV-Cre and all were sacrificed at 7 weeks. (B-D) Quantifications of liver to body weight ratios, relative tumor area, and absolute tumor load of these mice. (E) From left to right: Schematics depicting mosaic of genotypes where shade of green indicates levels of Yap/Taz activity; whole liver pictures (scale bar 1cm); liver sections stained with haematoxylin-eosin (H&E) (scale bar 1mm) and for HNFα^{+} (hepatocytes, red) and DAPI (white) (scale bar 500μm). (F-G) Ki67 staining (red) to detect proliferating cells and its quantification. Tumor cells are marked in green (anti-HA-tag). Scale bar 100μm. Data are mean ± SEM. * = p<0.05, ** = p<0.01, *** = p<0.001; n.s. = not significant.

Fig. 3. Hyperactivation of Yap/Taz in peritumoral hepatocytes causes tumor elimination.

(A) Experimental outline: *Lats1*$^{fl/fl}$*;Lats2*$^{fl/fl}$ mice were hydrodynamically injected with *N*^{ICD}*, HA-Akt* and *SB11* plasmids. After four weeks, half of these mice were injected with AAV-Cre and all were sacrificed at 6 weeks. (B-D) Quantifications of liver to body weight ratio, absolute tumor load, and evolution of tumor load in these mice. p = 000113 (E) From left to right: Schematics depicting mosaic of genotypes where shade of green indicates levels of Yap/Taz activity; whole liver pictures (scale bar 1cm); liver sections stained with haematoxylin-eosin (H&E) (scale bar 1mm) and for tumor cells (HA-Akt expression, green) and nuclei (DAPI, blue). Scale bar 500μm. (F) Evolution of tumor load. p = 0.028 (G) Survival of mice after two weeks of Dox. Data are mean ± SEM. * = p<0.05, ** = p<0.01, *** = p<0.001; n.s. = not significant.

Fig. 4. Tumor cell survival depends on Yap/Taz levels in surrounding tissue.

(A,B) TUNEL staining (green) and its quantification of liver sections of wild-type and *Lats1/2*^{CKO} mice with N-Akt tumors 6 days after AAV-Cre administration. Tumor cells are visualized by HA-Akt expression (red). Scale bars 100μm. (C) Western blots of lysates of tumors dissected from wild-type and *Lats1/2*^{CKO} livers detecting markers of apoptosis and nutrient status. (D) Western blots of tumor and whole liver lysates for Yap, Taz, and cleaved Caspase 3. Liver injury (CCl_4) was used as positive control for cell death markers. (E) From left to right: Schematics depicting mosaic of genotypes of *Yap*$^{fl/fl}$*;Taz*$^{fl/fl}$ mice hydrodynamically injected with *N*^{ICD}*, HA-Akt, SB11* together with or without *SB-Cre*^{ERT2}. At 4 weeks a portion of these mice received tamoxifen (5 consecutive days) together with or without AAV-Cre and all were sacrificed at 7 weeks. Whole liver pictures (scale bar 1cm), liver sections stained with haematoxylin-eosin (H&E) (scale bar 1mm) and for tumor cells (HA-Akt expression, green) and nuclei (DAPI, blue). Scale bar 500μm.

(F-H) Quantifications of liver to body weight ratios, relative tumor area, and absolute tumor load of these mice. (I-L) Myc-Ras HCC and *NRas-INK4a*$^{-}$ melanoma cells growing in *Apo>hYAP*^{1SA} mice with and without Dox administration starting 4 weeks after tumor initiation. Mice were sacrificed and analysed at 6 weeks. Whole liver pictures (scale bars 1cm) and tumor quantifications. Myc-Ras tumor cells were prevented to activate *Apo>hYAP*^{1SA} by expression of shRNAs targeting *rtTA* and *hYAP*^{1SA} (more details and controls in fig. S17, fig. S18, and fig. S19). Data are mean ± SEM. * = p<0.05, ** = p<0.01, *** = p<0.001; n.s. = not significant.

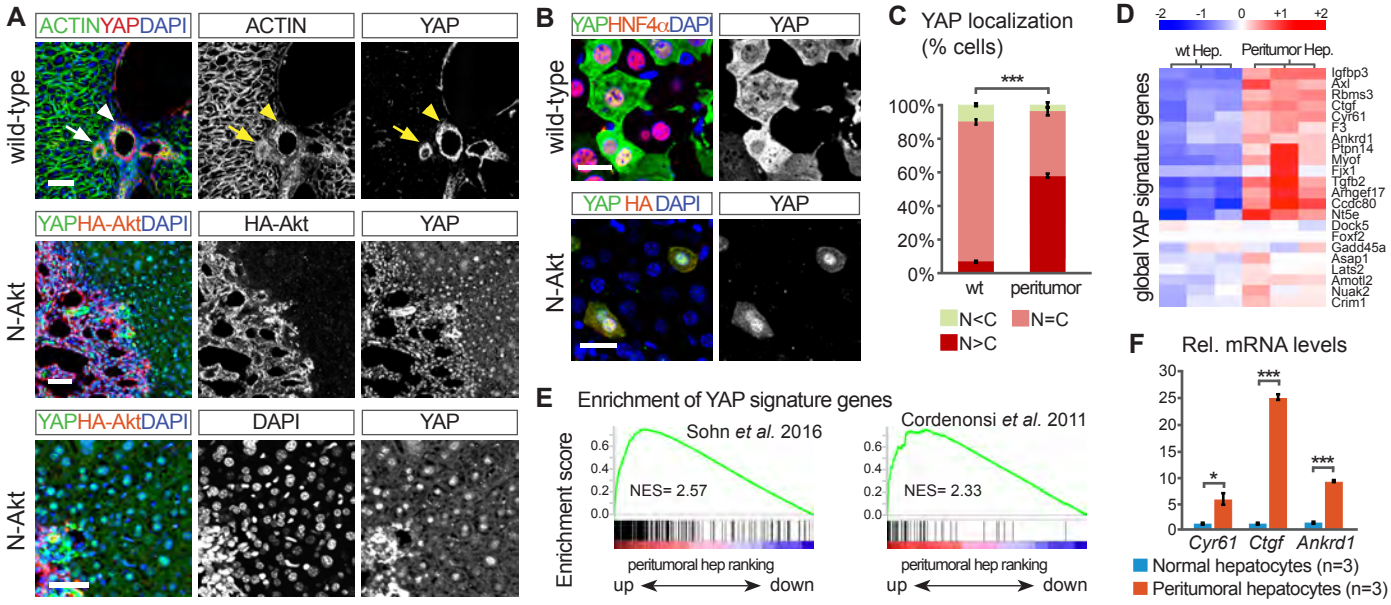
A
ACTINYAPDAPI
ACTIN
YAP
wild-type
YAPHA-AktDAPI
HA-Akt
YAP
N-Akt
YAPHA-AktDAPI
DAPI
YAP
N-Akt
B
YAPHNF4αDAPI
YAP
wild-type
YAP HA DAPI
YAP
N-Akt
C
YAP localization
(% cells)
***
100%
80%
60%
40%
20%
0%
wt
peritumor
N<C
N=C
N>C
D
-2
-1
0
+1
+2
wt Hep.
Peritumor Hep.
global YAP signature genes
Igfbp3
Axl
Rbms3
Ctgf
Cyr61
F3
Ankrd1
Ptpn14
Myof
Fjx1
Tgfb2
Arhgef17
Ccdc80
Nt5e
Dock5
Foxf2
Gadd45a
Asap1
Lats2
Amotl2
Nuak2
Crim1
E
Enrichment of YAP signature genes
Sohn et al. 2016
NES= 2.57
Cordenonsi et al. 2011
NES= 2.33
Enrichment score
0.6
0.4
0.2
0.0
peritumoral hep ranking
up
down
F
Rel. mRNA levels
30
25
20
15
10
5
0
*
***
***
Cyr61
Ctgf
Ankrd1
Normal hepatocytes (n=3)
Peritumoral hepatocytes (n=3)

Figure 1

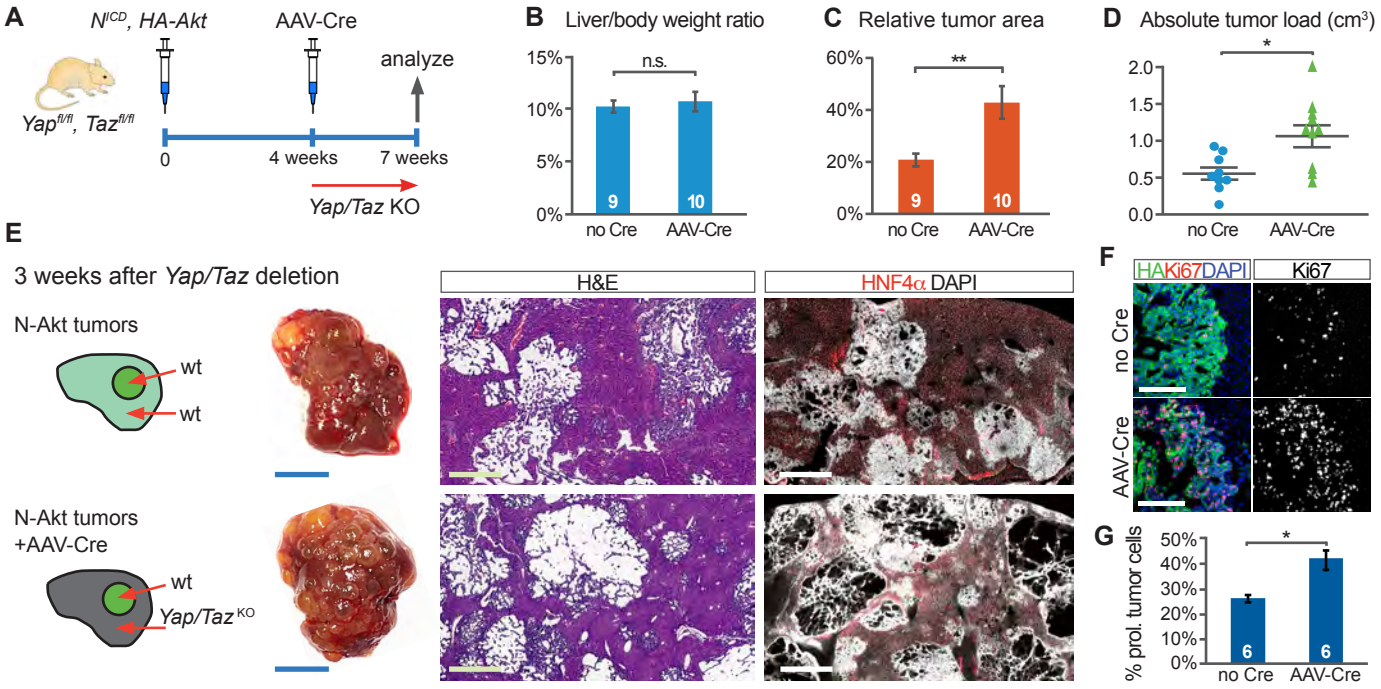
A
N^ICD, HA-Akt
AAV-Cre
analyze
Yap^fl/fl, Taz^fl/fl
0
4 weeks
7 weeks
Yap/Taz KO
B
Liver/body weight ratio
15%
10%
5%
0%
n.s.
9
10
no Cre
AAV-Cre
C
Relative tumor area
60%
40%
20%
0%
**
9
10
no Cre
AAV-Cre
D
Absolute tumor load (cm³)
2.0
1.5
1.0
0.5
0.0
*
no Cre
AAV-Cre
E
3 weeks after Yap/Taz deletion
N-Akt tumors
wt
wt
N-Akt tumors
+AAV-Cre
wt
Yap/Taz KO
H&E
HNF4α DAPI
F
HAKi67DAPI
Ki67
no Cre
AAV-Cre
G
% prol. tumor cells
50%
40%
30%
20%
10%
0%
*
6
6
no Cre
AAV-Cre

Figure 2

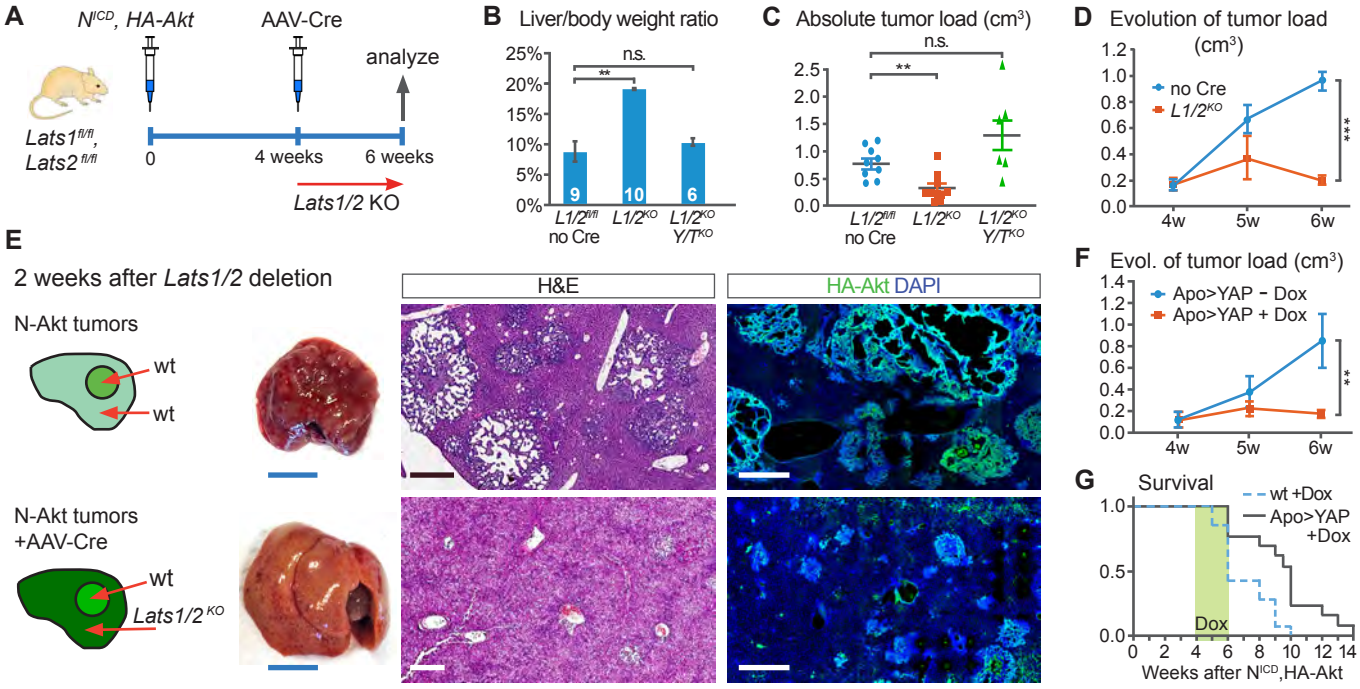
A
N^ICD, HA-Akt
AAV-Cre
analyze
Lats1^fl/fl, Lats2^fl/fl
0
4 weeks
6 weeks
Lats1/2 KO
B
Liver/body weight ratio
25%
20%
15%
10%
5%
0%
n.s.
**
9
10
6
L1/2^fl/fl no Cre
L1/2^KO
L1/2^KO Y/T^KO
C
Absolute tumor load (cm³)
n.s.
**
2.5
2.0
1.5
1.0
0.5
0.0
L1/2^fl/fl no Cre
L1/2^KO
L1/2^KO Y/T^KO
D
Evolution of tumor load (cm³)
1.2
1.0
0.8
0.6
0.4
0.2
0.0
no Cre
L1/2^KO
***
4w
5w
6w
E
2 weeks after Lats1/2 deletion
N-Akt tumors
wt
wt
N-Akt tumors +AAV-Cre
wt
Lats1/2^KO
H&E
HA-Akt DAPI
F
Evol. of tumor load (cm³)
1.4
1.2
1.0
0.8
0.6
0.4
0.2
0.0
Apo>YAP - Dox
Apo>YAP + Dox
**
4w
5w
6w
G
Survival
1.0
0.5
0.0
wt +Dox
Apo>YAP +Dox
Dox
0
2
4
6
8
10
12
14
Weeks after N^ICD,HA-Akt

Figure 3

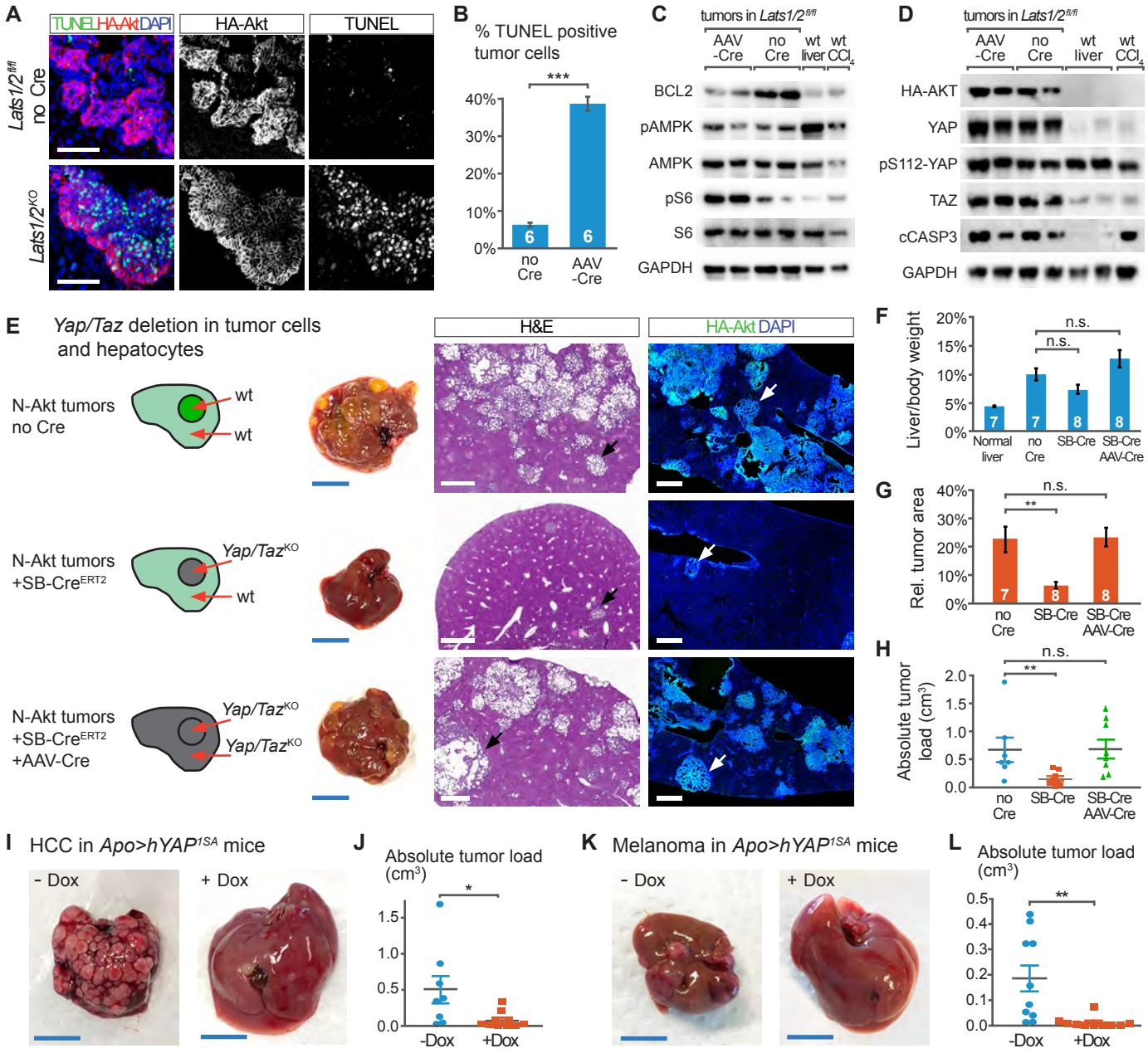
A
TUNEL HA-Akt DAPI
HA-Akt
TUNEL
Lats1/2fl/fl no Cre
Lats1/2KO
B
% TUNEL positive tumor cells
***
40%
30%
20%
10%
0%
6
6
no Cre
AAV -Cre
C
tumors in Lats1/2fl/fl
AAV -Cre
no Cre
wt liver
wt CCl4
BCL2
pAMPK
AMPK
pS6
S6
GAPDH
D
tumors in Lats1/2fl/fl
AAV -Cre
no Cre
wt liver
wt CCl4
HA-AKT
YAP
pS112-YAP
TAZ
cCASP3
GAPDH
E
Yap/Taz deletion in tumor cells and hepatocytes
H&E
HA-Akt DAPI
N-Akt tumors no Cre
wt
wt
N-Akt tumors +SB-CreERT2
Yap/TazKO
wt
N-Akt tumors +SB-CreERT2 +AAV-Cre
Yap/TazKO
Yap/TazKO
F
Liver/body weight
20%
15%
10%
5%
0%
n.s.
n.s.
7
7
8
8
Normal liver
no Cre
SB-Cre
SB-Cre AAV-Cre
G
Rel. tumor area
40%
30%
20%
10%
0%
n.s.
**
7
8
8
no Cre
SB-Cre
SB-Cre AAV-Cre
H
Absolute tumor load (cm3)
2.0
1.5
1.0
0.5
0.0
n.s.
**
no Cre
SB-Cre
SB-Cre AAV-Cre
I
HCC in Apo>hYAP1SA mice
- Dox
+ Dox
J
Absolute tumor load (cm3)
*
1.5
1.0
0.5
0.0
-Dox
+Dox
K
Melanoma in Apo>hYAP1SA mice
- Dox
+ Dox
L
Absolute tumor load (cm3)
**
0.5
0.4
0.3
0.2
0.1
0.0
-Dox
+Dox

Figure 4

Figure S1. Development of N-Akt cholangiocarcinoma in C57BL/6 mice.

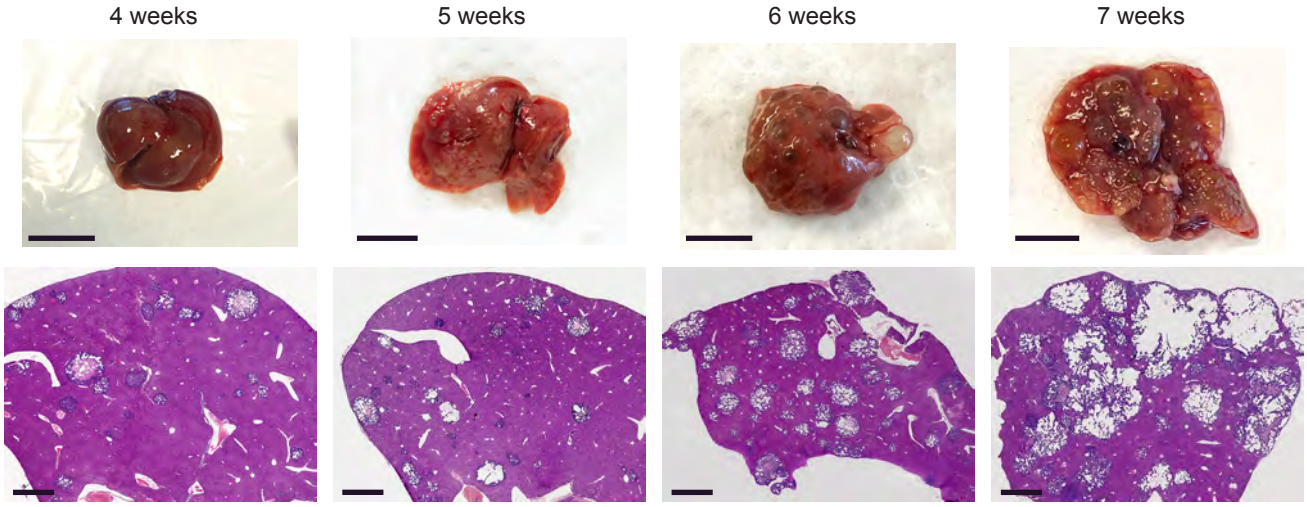

Figure S2. YAP nuclear localization is not triggered by single oncogene expression in peritumoral hepatocytes.

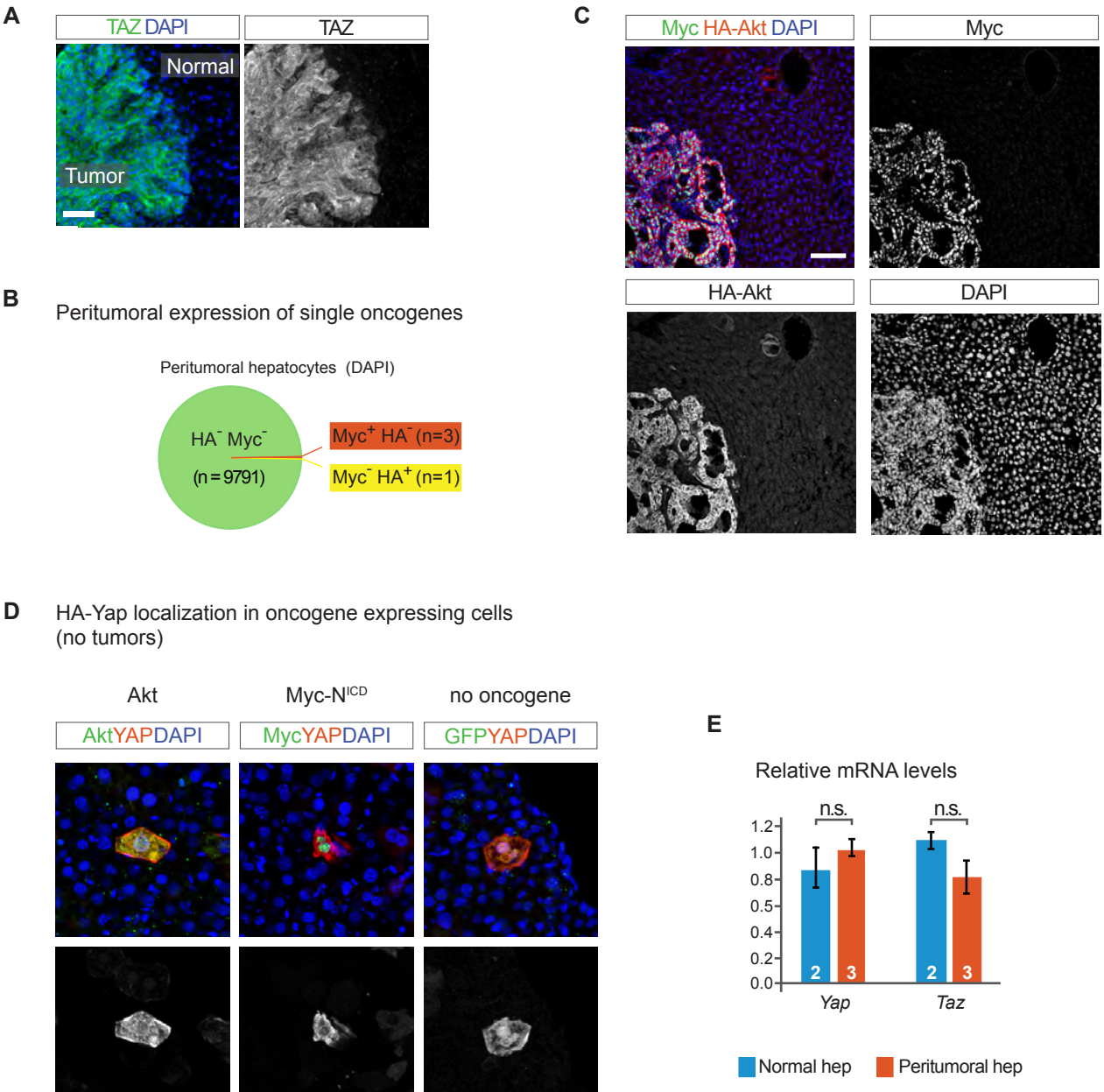

Figure S3. YAP and TAZ localization in human peritumoral hepatocytes.

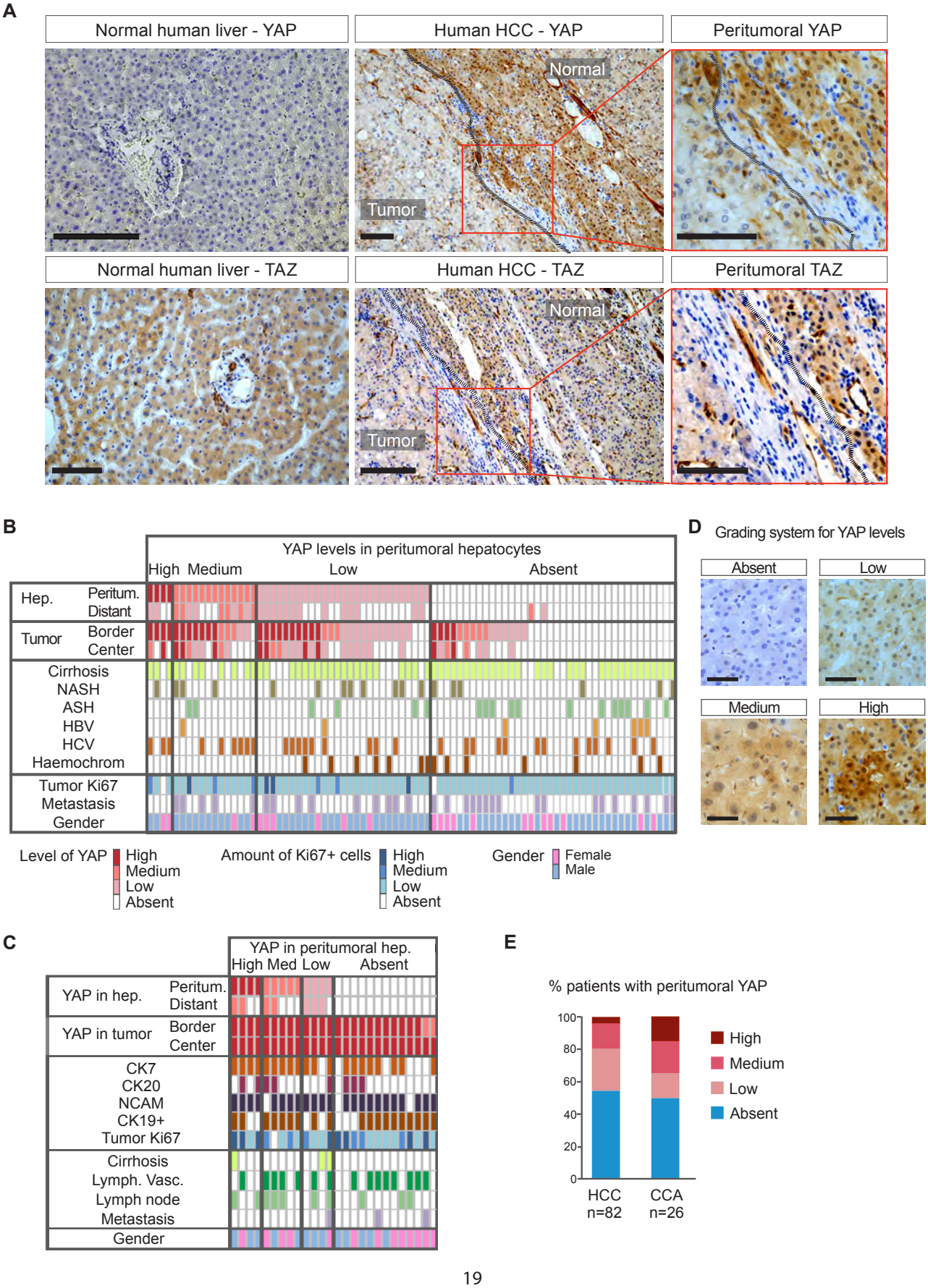

Figure S4. Intracellular localization of YAP in hepatocytes around human HCC.

A

Patterns of YAP localization in peritumoral hepatocytes

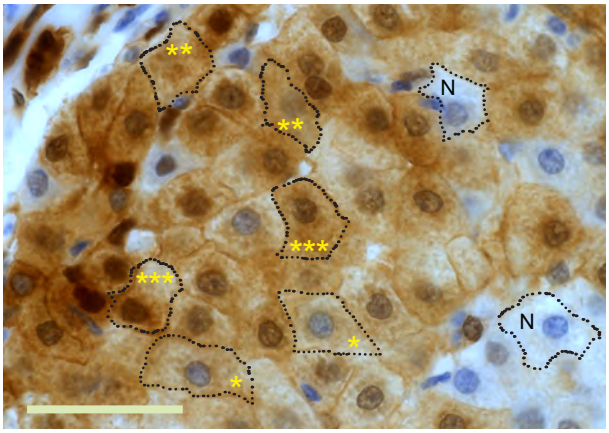

*** N>C

** N=C

* N<C

N Negative

B

YAP localization in peritumoral hepatocytes around human HCC tumors

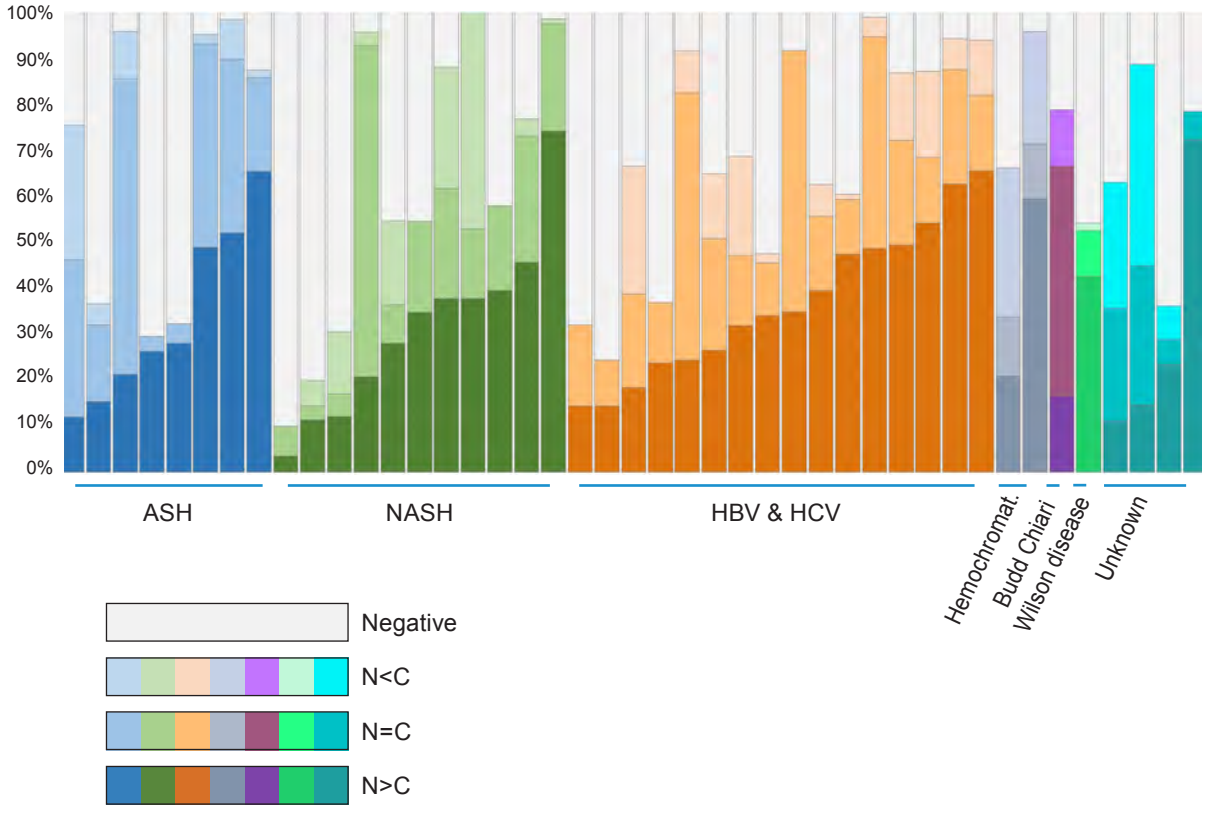

Figure S5. Accumulation of YAP in hepatocytes around metastatic tumors derived from melanoma and colorectal cancer.

A Human melanoma metastases to the liver

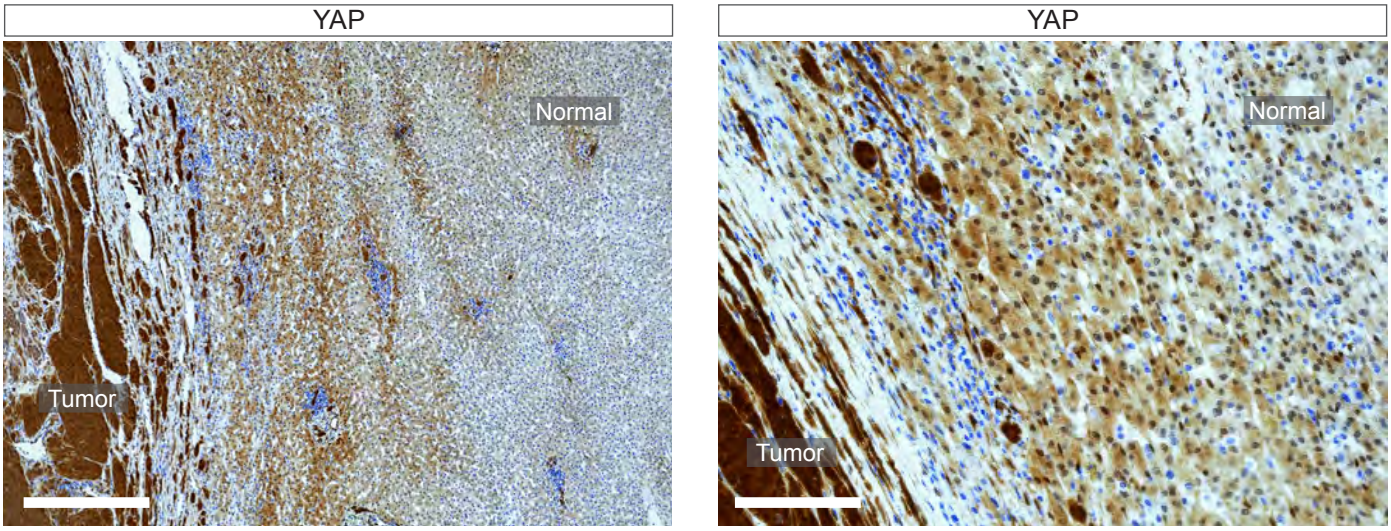

B Human colorectal cancer metastases to the liver

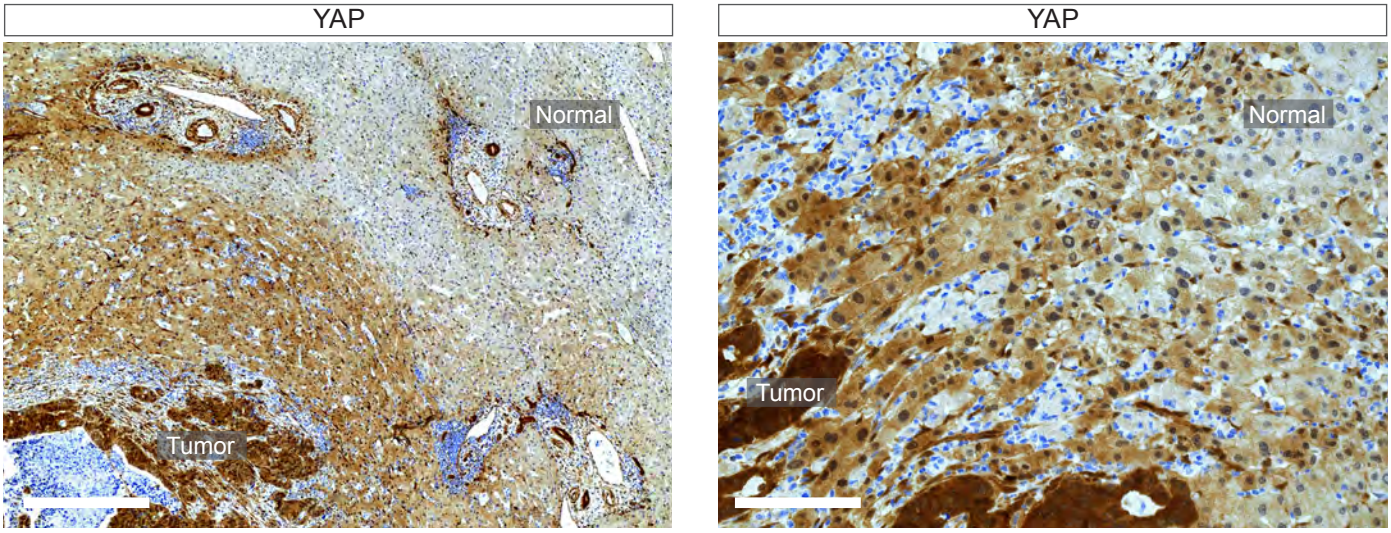

Figure S6. Isolation of peritumoral hepatocytes for RNA-seq.

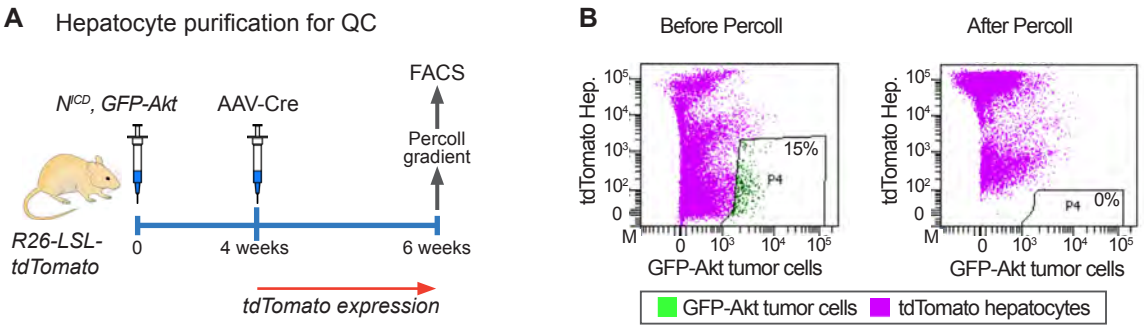

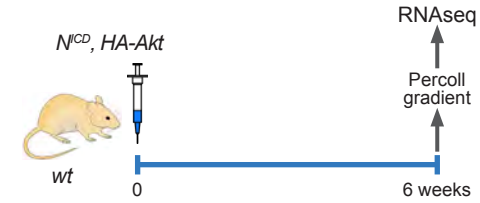

D

GO-terms	p-value
Regulation of cell proliferation	8.7E-30
Angiogenesis	4.1E-22
Regulation of cell death	3.3E-14
Tissue morphogenesis	2.6E-14
Immune response	6.7E-13
Response to stress	2.9E-12
Response to wounding	9.0E-11

Figure S7. Proliferation of peritumoral hepatocytes around N-Akt tumors in mice.

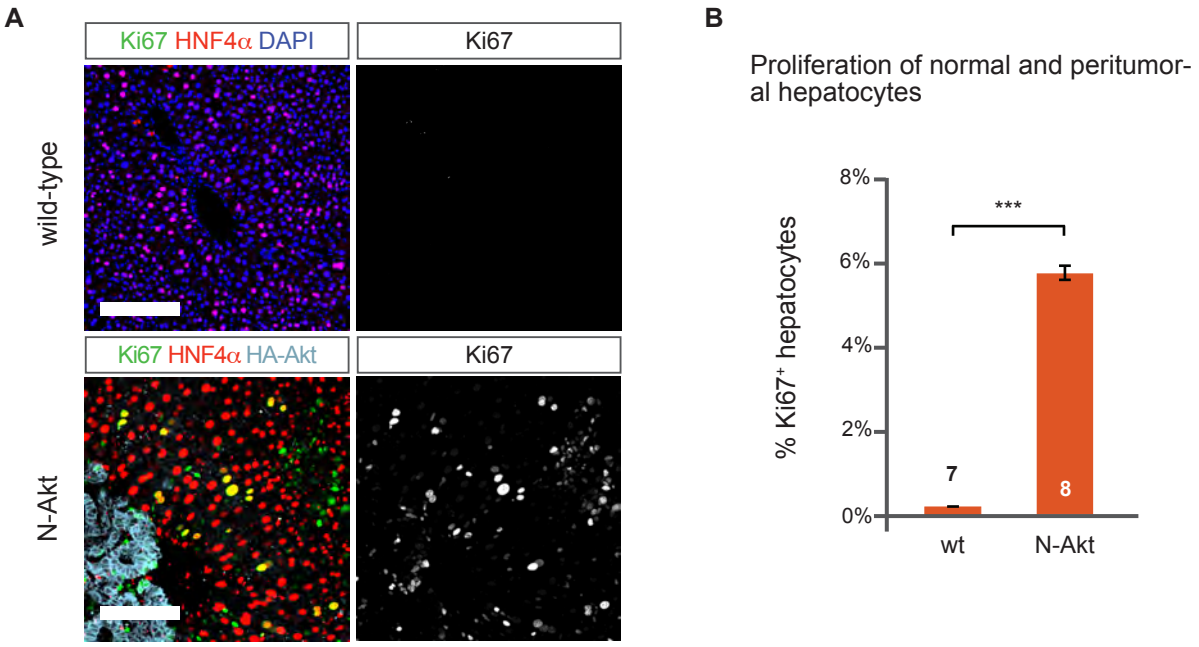

Figure S8. Recombination efficiency and specificity of AAV-Cre in peritumoral hepatocytes.

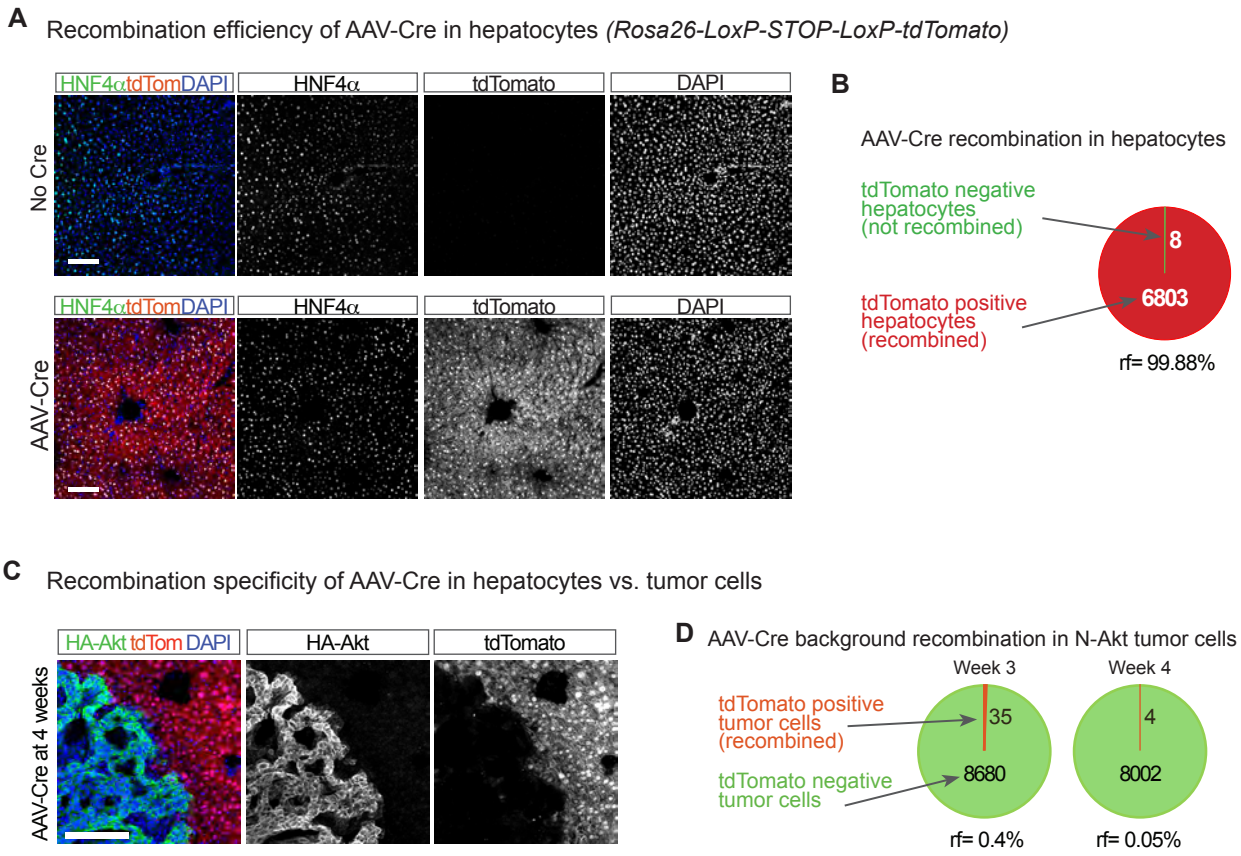

Figure S9. Effect of Cre expression in tumor cells or peritumoral hepatocytes on N-Akt tumor load in wild-type mice.

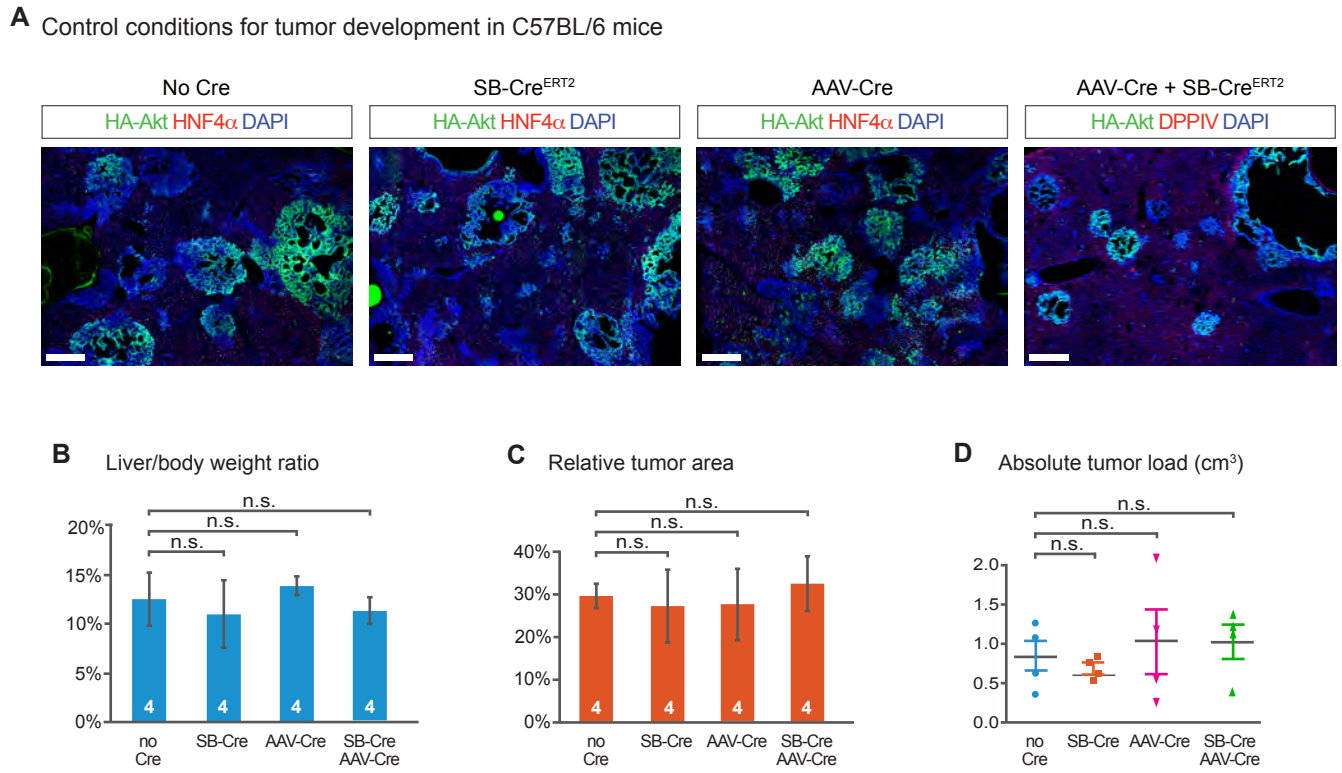

Figure S10. YAP and TAZ mediate the tumor elimination effect triggered by *Lats1/2* deletion in peritumoral hepatocytes.

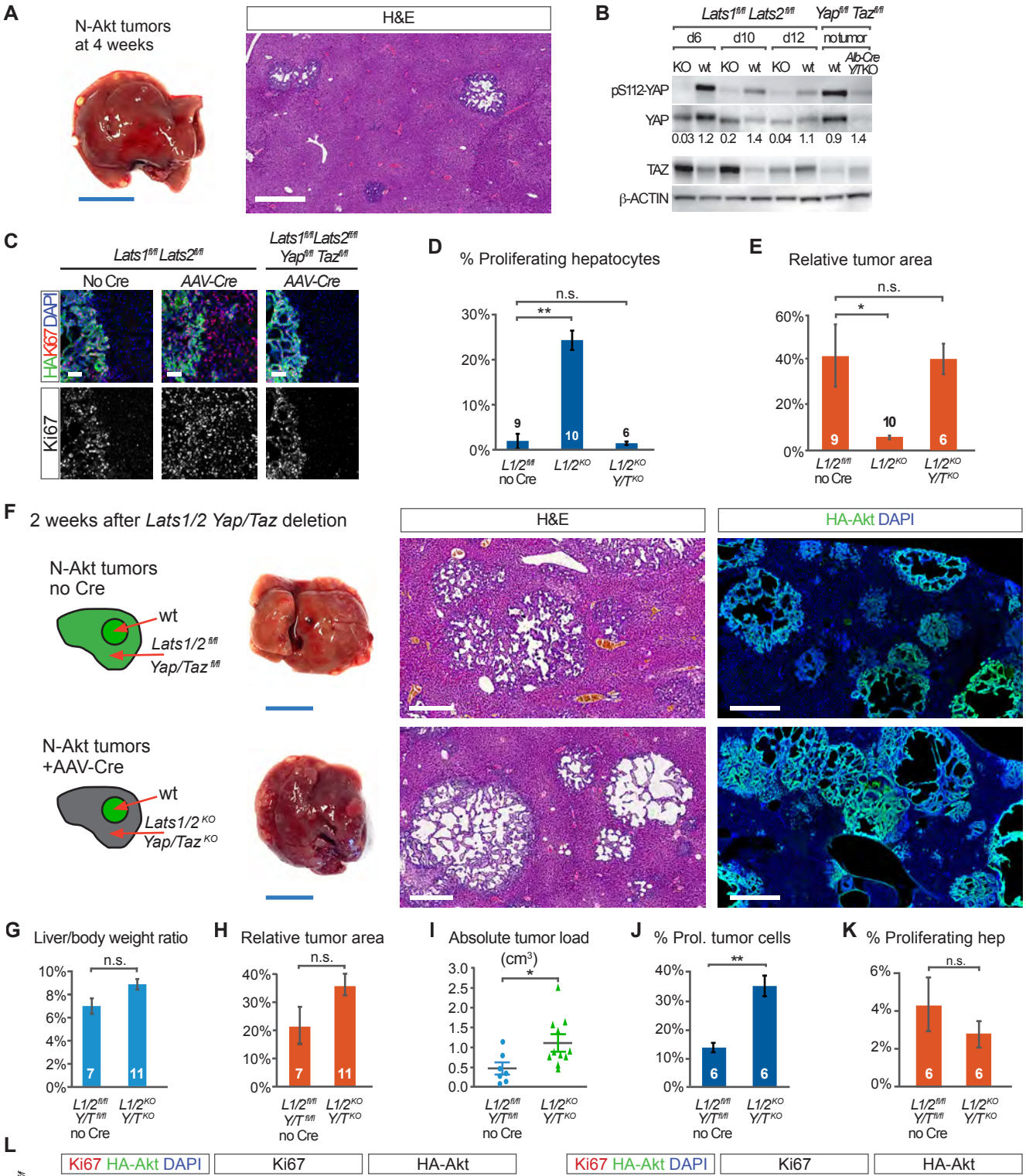

Figure S11. Overexpression of YAP^{1SA} in peritumoral hepatocytes triggeres tumor elimination.

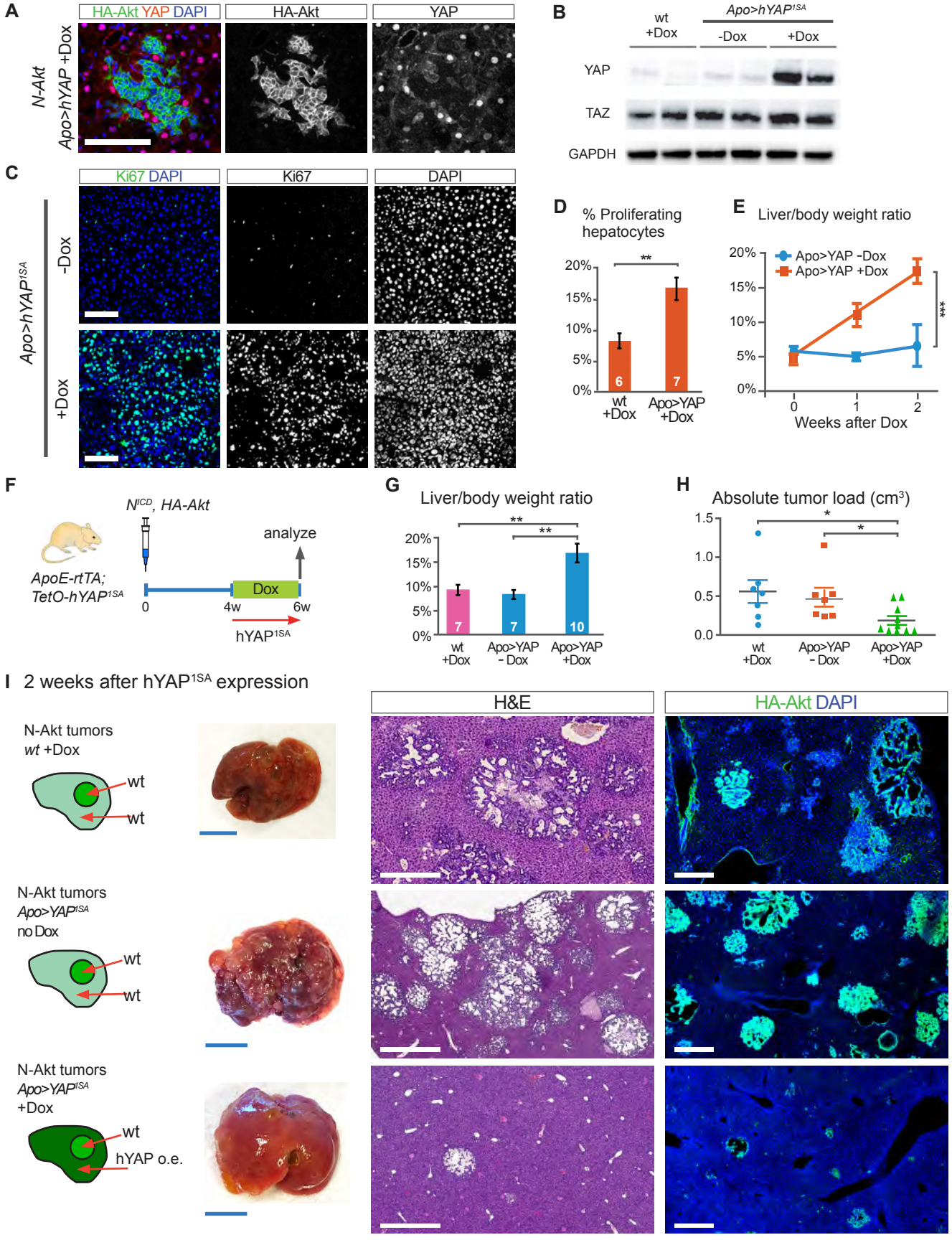

Figure S12. Hepatocyte hyperproliferation caused by deleting *PTEN* and overexpressing BRAF^{V600E} did not trigger tumor elimination.

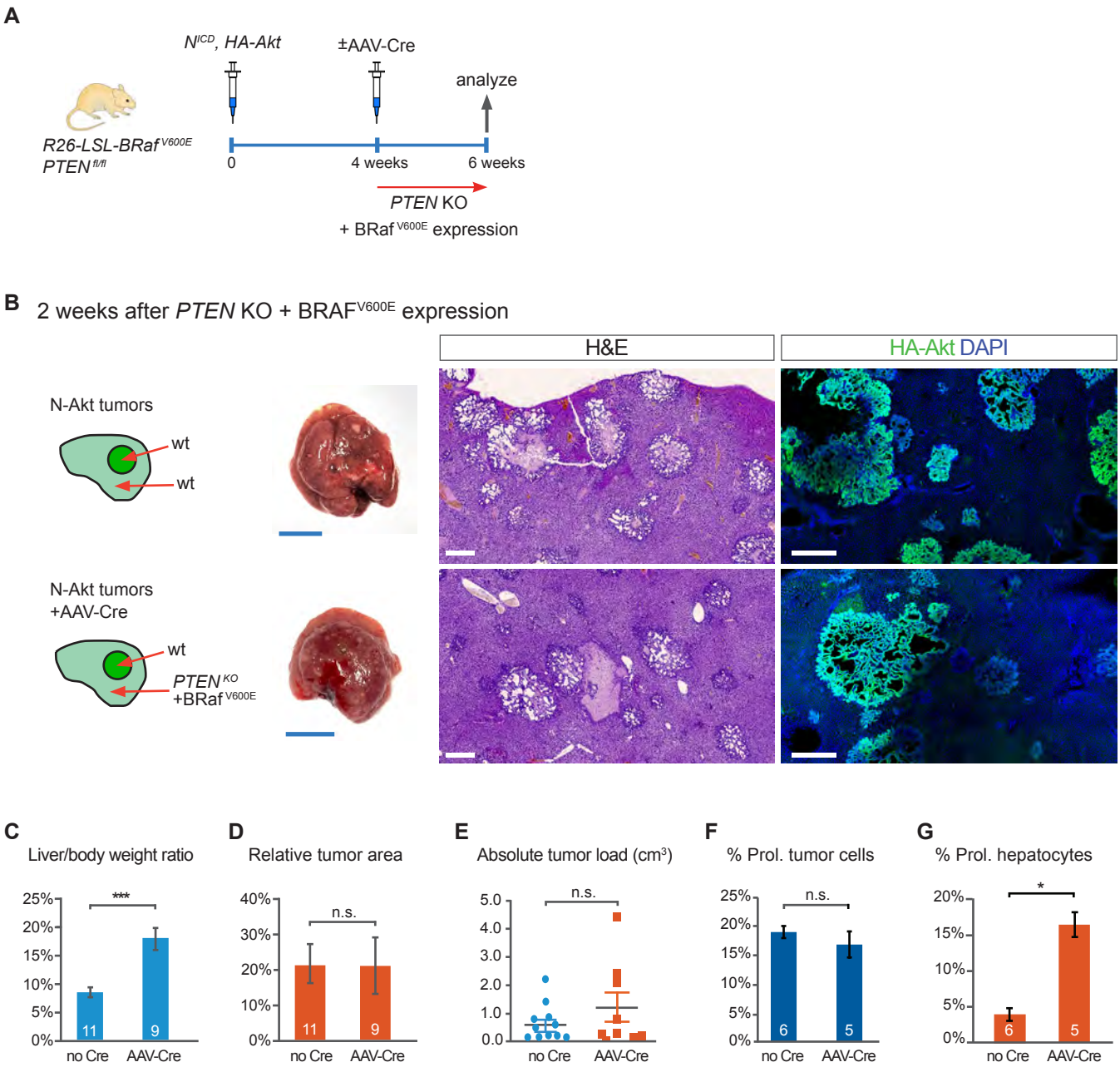

Figure S13. Analysis of cell death pathways in tumors eliminated by peritumoral activation of YAP.

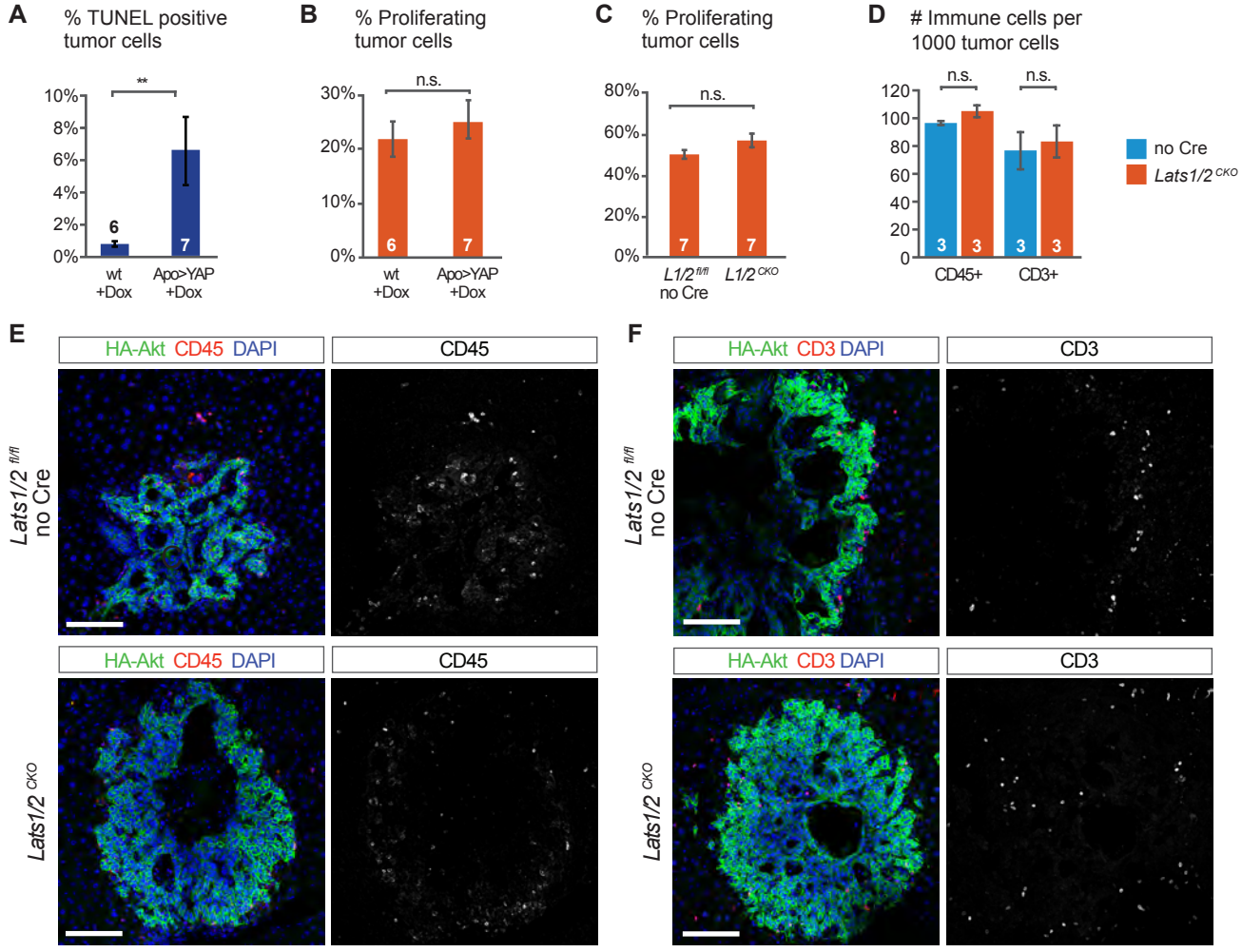

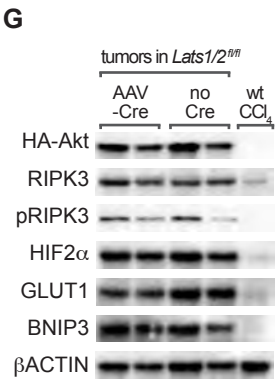

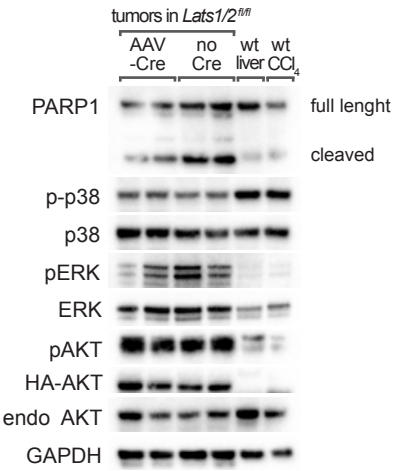

Figure S14. BCL2 overexpression in tumor cells suppressed tumor elimination triggered by peritumoral deletion of *Lats1/2*.

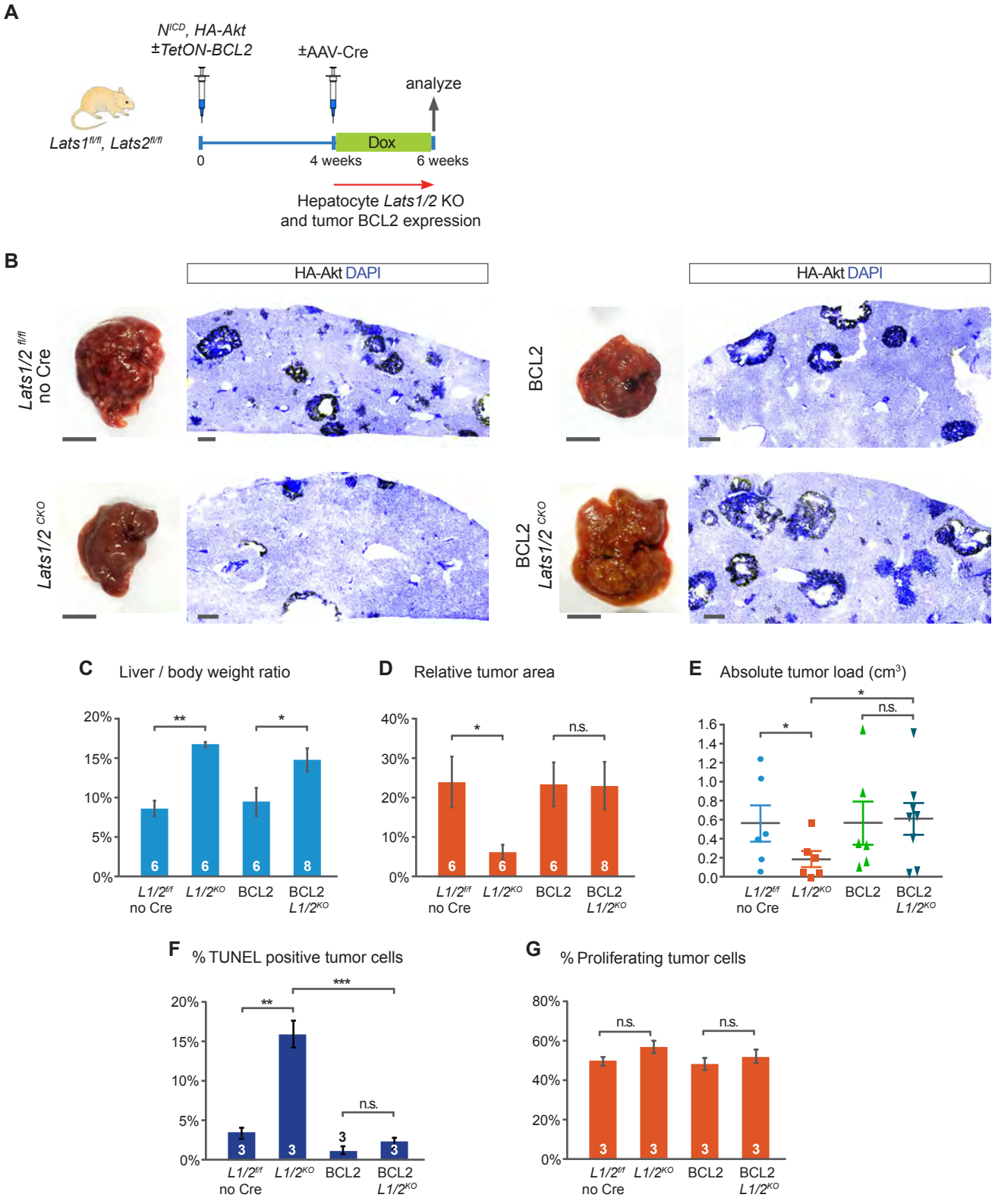

Figure S15. BCL2 overexpression in tumor cells suppressed tumor elimination triggered by peritumoral expression of hYap^{1SA}.

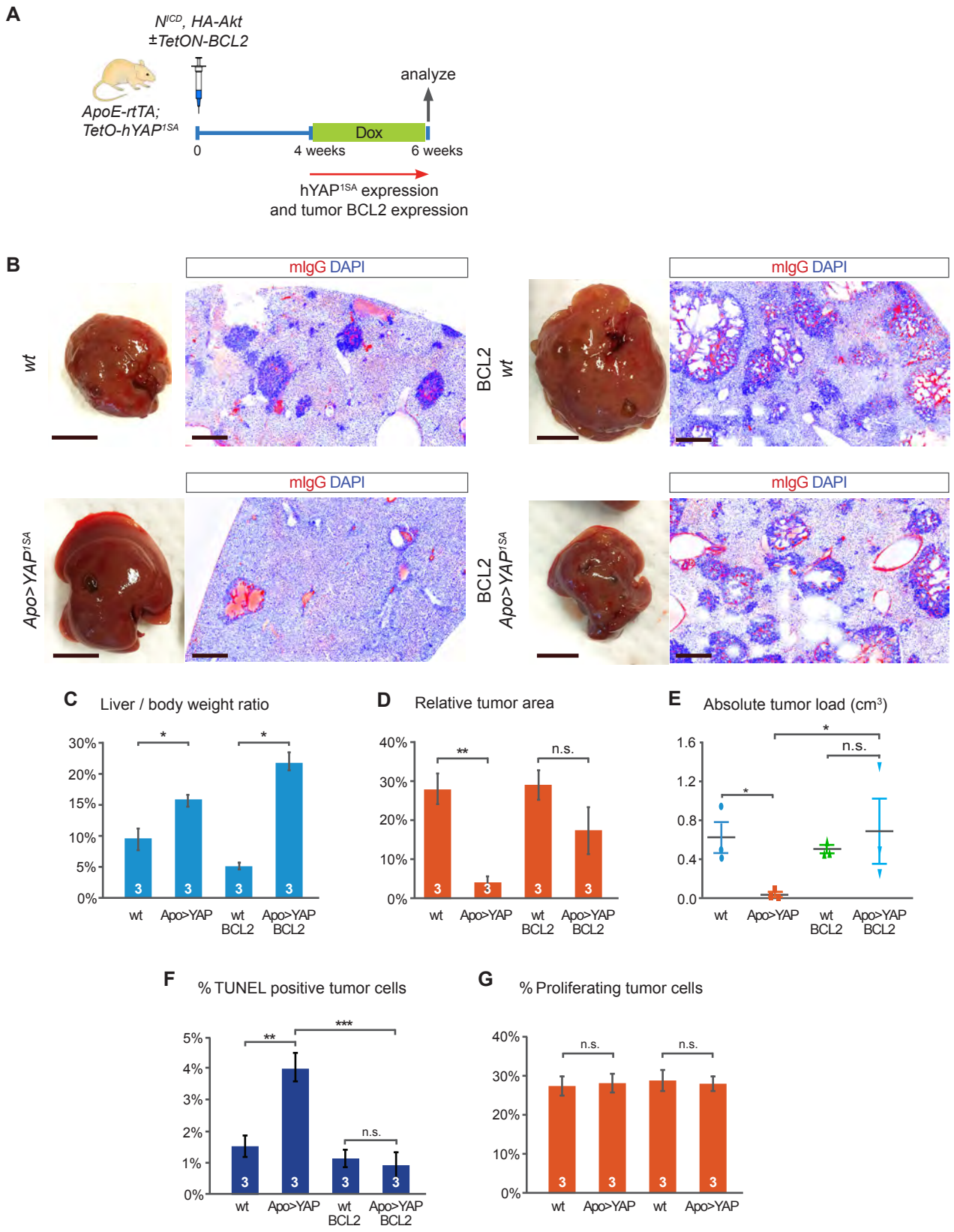

Figure S16. Validation of Cre expression in tumor cells and peritumoral hepatocytes.

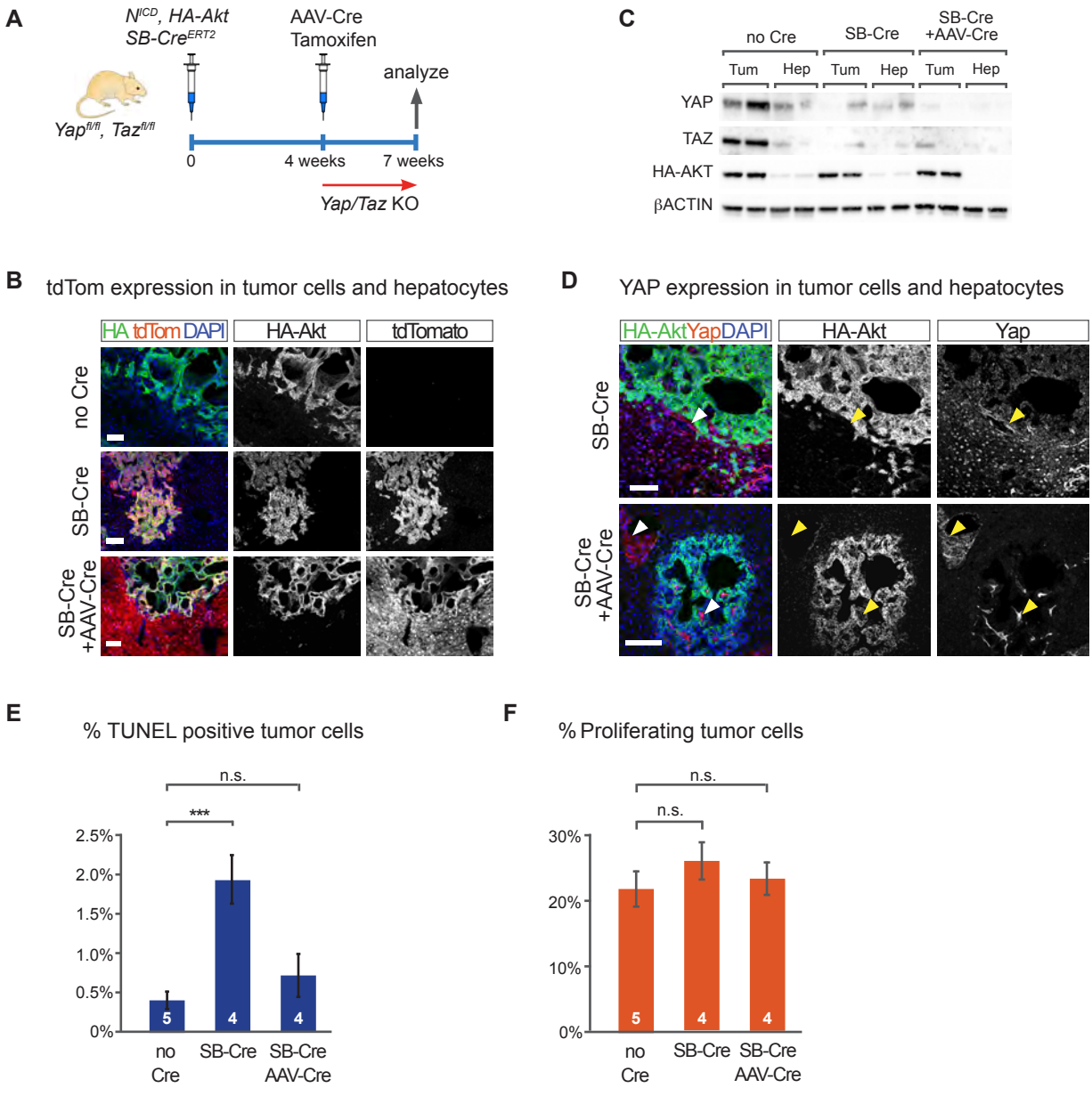

Figure S17. Peritumoral expression of hYAP^{1SA} eliminates Myc-Ras tumors.

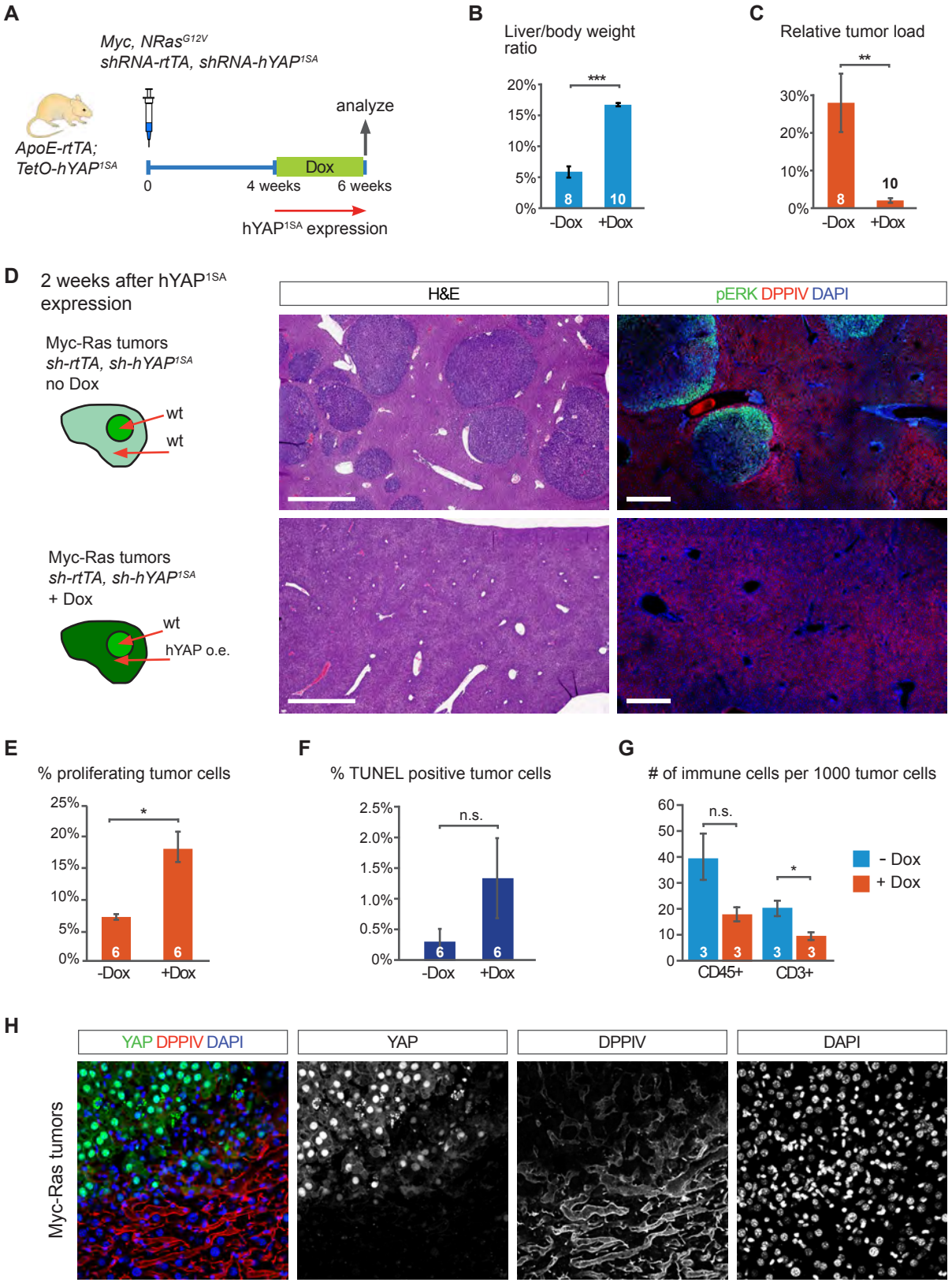

Figure S18. shRNA controls and additional conditions for the experiment of expressing hYAP^{1SA} in hepatocytes around Myc-Ras tumors.

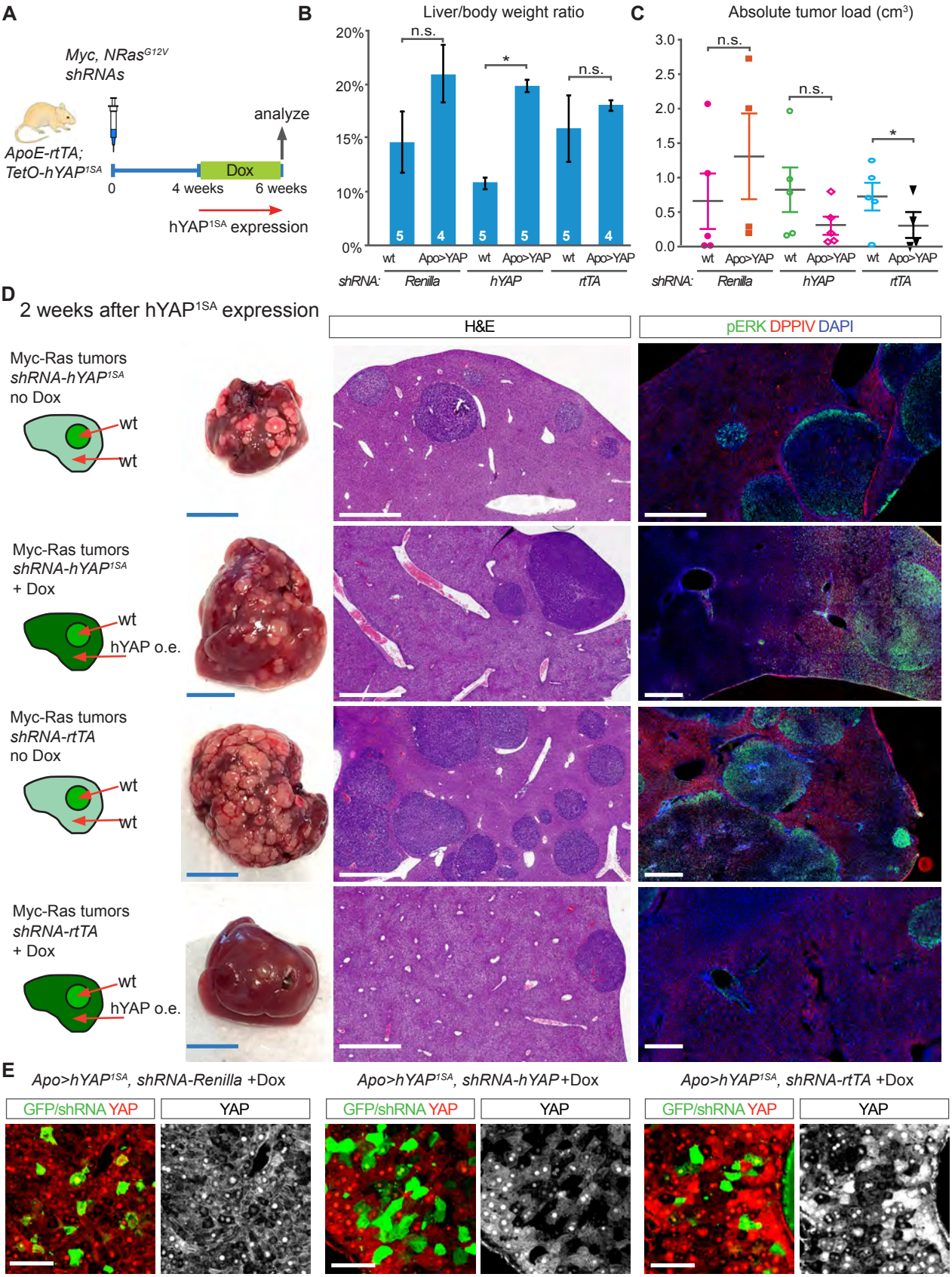

Figure S19. Peritumoral expression of hYAP^{1SA} eliminates melanoma metastases in mouse livers.